

ALS-linked mutant SOD1 induces ER stress- and ASK1-dependent motor neuron death by targeting Derlin-1

Hideki Nishitoh,^{1,2,3} Hisae Kadowaki,^{1,2,3,4,5} Atsushi Nagai,³ Takeshi Maruyama,³ Takanori Yokota,⁶ Hisashi Fukutomi,^{1,4,5} Takuya Noguchi,^{1,4,5} Atsushi Matsuzawa,^{1,4,5} Kohsuke Takeda,^{1,4,5} and Hidenori Ichijo^{1,4,5,7}

¹Core Research for Evolutional Science and Technology (CREST), Japan Science and Technology Corporation, Bunkyo-ku, Tokyo 113-0033, Japan, ²Oral and Maxillofacial Surgery, Graduate School, Tokyo Medical and Dental University, Bunkyo-ku, Tokyo 113-8510, Japan, ³Center of Excellence Program for Frontier Research on Molecular Destruction and Reconstruction of Tooth and Bone, Tokyo Medical and Dental University, Bunkyo-ku, Tokyo 113-8510, Japan, ⁴Cell Signaling, Graduate School of Pharmaceutical Sciences, The University of Tokyo, Bunkyo-ku, Tokyo 113-0033, Japan, ⁵Strategic Approach to Drug Discovery and Development in Pharmaceutical Sciences, Center of Excellence Program, Bunkyo-ku, Tokyo 113-0033, Japan, ⁶Department of Neurology and Neurological Science, Graduate School, Tokyo Medical and Dental University, Bunkyo-ku, Tokyo 113-8519, Japan

Mutation in *Cu/Zn-superoxide dismutase (SOD1)* is a cause of familial amyotrophic lateral sclerosis (ALS). Mutant SOD1 protein (SOD1^{mut}) induces motor neuron death, although the molecular mechanism of SOD1^{mut}-induced cell death remains controversial. Here we show that SOD1^{mut} specifically interacted with Derlin-1, a component of endoplasmic reticulum (ER)-associated degradation (ERAD) machinery and triggered ER stress through dysfunction of ERAD. SOD1^{mut}-induced ER stress activated the apoptosis signal-regulating kinase 1 (ASK1)-dependent cell death pathway. Perturbation of binding between SOD1^{mut} and Derlin-1 by Derlin-1-derived oligopeptide suppressed SOD1^{mut}-induced ER stress, ASK1 activation, and motor neuron death. Moreover, deletion of *ASK1* mitigated the motor neuron loss and extended the life span of SOD1^{mut} transgenic mice. These findings demonstrate that ER stress-induced ASK1 activation, which is triggered by the specific interaction of Derlin-1 with SOD1^{mut}, is crucial for disease progression of familial ALS.

[**Keywords:** Amyotrophic lateral sclerosis; endoplasmic reticulum-associated degradation; endoplasmic reticulum stress; Derlin-1; ASK1]

Supplemental material is available at <http://www.genesdev.org>.

Received December 5, 2007; revised version accepted April 11, 2008.

Amyotrophic lateral sclerosis (ALS) is the most frequent adult-onset motor neuron disease and is characterized by selective loss of motor neurons. Familial ALS-linked mutations of *Cu/Zn-superoxide dismutase (SOD1)* induce motor neuron death. Previous studies have suggested that SOD1^{mut} causes various cellular events, including alteration of gene expression (Yoshihara et al. 2002; Kirby et al. 2005), abnormal protein interactions (Kunst et al. 1997), activation of caspases (Pasinelli et al. 1998; Li et al. 2000), dysfunction of mitochondria (Bowling et al. 1993; Wong et al. 1995; Liu et al. 2004), and cytoskeletal abnormalities (Julien and Beaulieu 2000). However, the causal relationship between these events and motor neuron death remains unclear.

Endoplasmic reticulum (ER) stress is triggered by the

accumulation of misfolded proteins within the ER lumen and has recently been implicated in various neurodegenerative diseases (Sekine et al. 2006). Recent studies have suggested that ER stress signaling is also involved in the pathogenesis of ALS (Tobisawa et al. 2003; Atkin et al. 2006; Kikuchi et al. 2006). We showed previously that, upon ER stress, an ER-resident type I transmembrane serine/threonine kinase termed IRE1 recruits TRAF2 and ASK1 (apoptosis signal-regulating kinase 1) on the ER membrane and thus activates the ASK1-dependent apoptosis pathway (Nishitoh et al. 2002). Several groups have reported that activation of the ASK1 cascade is associated with induction of motor neuron death by SOD1^{mut} both in vitro (Raoul et al. 2002) and in vivo (Wengenack et al. 2004; Holasek et al. 2005; Vegliane et al. 2006). These observations suggested that a functional link between ER stress and ASK1 may exist in the process of SOD1^{mut}-induced motor neuron death. However, the molecular mechanism by which SOD1^{mut}

⁷Corresponding author.

E-MAIL ichijo@mol.f.u-tokyo.ac.jp; FAX 81-3-5841-4778.
Article is online at <http://www.genesdev.org/cgi/doi/10.1101/gad.1640108>.

Nishitoh et al.

induces ER stress has remained unclear. Furthermore, genetic evidence has not been provided regarding the hypothetical involvement of ER stress-ASK1 pathway in SOD1^{mut}-induced motor neuron death. In the present study, we investigated the molecular mechanism of SOD1^{mut}-induced ER stress and the role of ER stress-induced ASK1 activation in the pathogenesis of ALS.

Results

SOD1^{mut} triggers ER stress

To investigate the causal relationship between SOD1^{mut} and ER stress-dependent motor neuron death, we first examined whether SOD1^{mut} induces ER stress in NSC34 motor neurons, as assessed by band-shift analyses of the ER transmembrane kinase receptors IRE1 and PERK. Adenovirus (Ad)-mediated expression of ALS-linked SOD1^{mut} (SOD1^{C93A}) was detectable within 48 h of infection (Supplemental Fig. S1A). SOD1^{mut} (SOD1^{A4V}, SOD1^{G85R}, and SOD1^{C93A}) but not wild-type SOD1 (SOD1^{wt}) activated IRE1 and PERK (Fig. 1A; Supplemental Fig. S1A). To confirm the activation of IRE1 by SOD1^{mut}, we examined Xbp-1 mRNA splicing by RT-PCR. We clearly observed the appearance of spliced Xbp-1 mRNA by SOD1^{mut} but not SOD1^{wt} in HEK293 cells (Supplemental Fig. S1B) and NSC34 cells (Fig. 4D, lanes 2–5, below). SOD1^{mut}-specific induction of CHOP and BiP (ER stress marker proteins) was also observed (Fig. 1B). These findings suggested that accumulation of various SOD1^{mut} proteins commonly induce ER stress.

Inhibition of proteasome activity has been reported to be induced by SOD1^{mut} in Neuro2a cells (Urushitani et al. 2002). Since polyglutamine (polyQ) fragments have been shown to induce ER stress through inhibition of proteasome activity (Nishitoh et al. 2002), SOD1^{mut} might also induce ER stress through proteasomal dysfunction. We therefore examined whether alteration of proteasome activity was involved in SOD1^{mut}-induced ER stress. Proteasome activity was inhibited by treatment with lactacystin, a proteasome inhibitor, but not by Ad-mediated expression of SOD1^{mut} in NSC34 cells within 48 h (Supplemental Fig. S2A). These findings suggested that a mechanism other than proteasomal dysfunction may be involved in SOD1^{mut}-induced ER stress in NSC34 cells.

SOD1^{mut} inhibits ERAD

Restoration of ER homeostasis is achieved mainly by two independent mechanisms, chaperone-dependent refolding and ER-associated degradation (ERAD). In ERAD, misfolded proteins are exported from the ER back into the cytosol and are rapidly degraded by the ubiquitin-proteasome system (UPS) (Kopito 1997; Tsai et al. 2002; Meusser et al. 2005). Blocking of the refolding mechanism and/or the ERAD mechanism induces accumulation of misfolded proteins within the ER lumen and thus ER stress. Since SOD1^{mut} clearly induced expression of

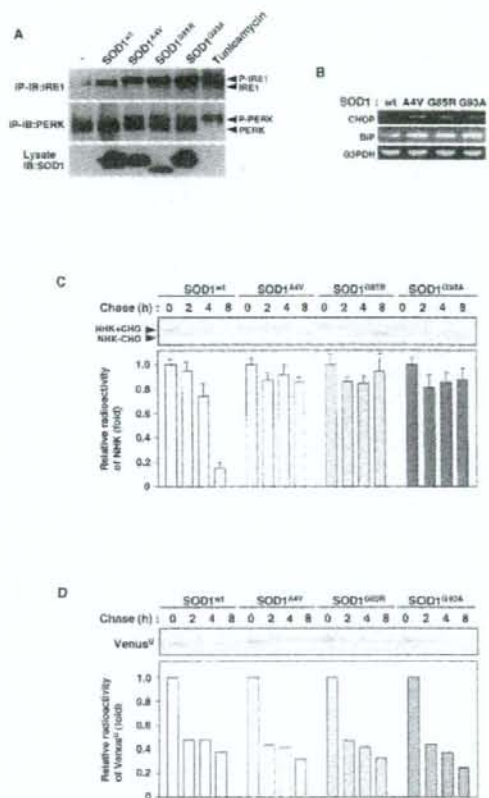


Figure 1. SOD1^{mut} triggers ER stress and inhibition of ERAD. [A] NSC34 cells were lysed after infection with Ad-SOD1^{wt}, Ad-SOD1^{A4V}, Ad-SOD1^{G85R}, or Ad-SOD1^{C93A} for 48 h or treatment with 2.5 μ g/mL tunicamycin (a potent inducer of ER stress) for 2 h and analyzed by immunoprecipitation-immunoblotting (IP-IB) with antibodies to IRE1 α or PERK. (P-IRE1) Activated IRE1, (P-PERK) activated PERK. The presence of SOD1 in the same lysates is shown. [B] NSC34 cells were transfected with SOD1^{wt} or SOD1^{mut} for 48 h. Expression of BiP and CHOP was examined by RT-PCR. [C] NSC34 cells were transfected with NHK and SOD1^{wt} or SOD1^{mut}. Cells were pulse-labeled with [³⁵S] methionine and cysteine and chased for the indicated time periods. Cell lysates were immunoprecipitated with antibody to α 1AT. (NHK + CHO) Glycosylated NHK, (NHK - CHO) deglycosylated NHK. The relative radioactivities in NHK at different times of chase were calculated and are shown as fold decreases relative to the intensity observed at 0 h chase. [D] NSC34 cells were transfected with Venus^U and SOD1^{wt} or SOD1^{mut}. Cells were pulse-labeled with [³⁵S] methionine and cysteine and chased for the indicated time periods. Cell lysates were immunoprecipitated with antibody to GFP. The relative radioactivities in Venus^U at different times of chase were calculated and are shown as fold decreases relative to the intensity observed at 0 h chase.

the ER-resident chaperone BiP (Fig. 1B), the productive refolding mechanism appears not to be inhibited by SOD1^{mut}. To examine whether SOD1^{mut} interferes with the ERAD mechanism, we examined the stability of the null Hong Kong (NHK) mutant protein of α 1-antitrypsin (α 1AT), an ER luminal misfolded protein (Sifers et al. 1988). Pulse-chase experiments showed that NHK was degraded with a half-life of <8 h in NSC34 cells transfected with or without SOD1^{wt} (Fig. 1C; Supplemental Fig. S3A). In contrast, overexpression of SOD1^{mut} decreased the degradation of NHK to a half-life of >8 h (Fig. 1C). To confirm the interference with the degradation of the other ERAD substrate by SOD1^{mut}, we examined the stability of CD38, a well-characterized transmembrane-type ERAD substrate (Fang et al. 2001). Cycloheximide chase experiments showed that the degradation of CD38 was also retarded by overexpression of SOD1^{mut} (Supplemental Fig. S3C). To further examine whether SOD1^{mut} also interferes with the degradation of cytosolic protein, we examined the stability of the unstable Venus mutant protein (Venus^U), a cytosolic proteasome substrate. There was no difference between a half-life of Venus^U in SOD1^{wt} transfected cells and that in SOD1^{mut} transfected cells (Fig. 1D). These findings suggested that SOD1^{mut} specifically impairs ERAD function but not cytosolic protein degradation in motor neurons. Furthermore, SOD1^{mut} clearly delayed the deglycosylation of NHK in addition to degradation (see the band shift of NHK; Fig. 1C). Previous studies have reported that the cytoplasmic peptide N-glycanase contributes to deglycosylation of misfolded glycoproteins prior to degradation (Suzuki et al. 2002). Thus, the delay of the deglycosylation of NHK suggested that SOD1^{mut} delays retro-translocation from ER lumen to the cytosol.

SOD1^{mut} interacts specifically with Derlin-1

Since inhibition of the UPS is unlikely to be essential for SOD1^{mut}-induced ER stress (Fig. 1D; Supplemental Fig. S2A), disturbance of the retro-translocation system from the ER lumen to the cytoplasm may be a potential target of SOD1^{mut}. Various proteins involved in ERAD have been identified recently (Meusser et al. 2005). Among them, components of the retro-translocation machinery including ATPase p97, its cofactors Ufd1 and Npl4, and the ER membrane proteins Derlin-1 and VIMP are of key importance to ERAD function (Lilley and Ploegh 2004; Ye et al. 2004). We therefore examined the *in vitro* interactions of SOD1^{mut} with p97, Ufd1, Npl4, VIMP, and Derlin-1. *In vitro*-translated ³⁵S-labeled Derlin-1, but not p97, Ufd1, Npl4, or VIMP, bound specifically to recombinant His-tagged SOD1^{G93A} (Fig. 2A). To examine the interaction of Derlin-1 with different mutant forms of SOD1, several SOD1 mutants, including the A4V, G85R, and G93A mutants, were analyzed in mammalian cells. SOD1^{A4V}, SOD1^{G85R}, and SOD1^{G93A}, but not SOD1^{wt}, were clearly coimmunoprecipitated with Derlin-1 (Fig. 2B). The remaining ERAD components, including p97, Npl4, Ufd1, and VIMP, were not coimmunoprecipitated with SOD1^{mut} (data not shown). The specific interaction

between exogenous SOD1^{mut} and endogenous Derlin-1 was also observed in NSC34 cells (Fig. 2C). These findings suggested that SOD1^{mut} proteins specifically interact with Derlin-1 in mammalian cells.

To confirm these results in more physiological conditions, we examined the association of endogenous Derlin-1 and SOD1 in spinal cord of SOD1^{G93A} gene transgenic (SOD1^{G93A}) mice. SOD1^{G93A} mice showed the onset of motor function loss, which was measured using rota-rod test, at a mean age of 28.1 \pm 1.3 wk, and died at a mean age of 34.9 \pm 1.6 wk (see below and Fig. 5G). Accumulation of SOD1^{mut} was observed in the spinal cord of SOD1^{G93A} mice at the post-onset stage and the end stage (Fig. 2D). A strong interaction of endogenous Derlin-1 with exogenous SOD1^{G93A}, but not with exogenous SOD1^{wt} (Supplemental Fig. S8A), was observed in parallel with accumulation of SOD1^{mut} (Fig. 2D).

The reported expression pattern of Derlin-1 in mouse organs is controversial (Lilley and Ploegh 2005; Oda et al. 2006). We thus examined whether Derlin-1 is expressed in neuronal tissues of SOD1^{wt} and SOD1^{G93A} mice by immunoblotting analysis using a newly developed Derlin-1-specific antibody (Supplemental Fig. S4A). Derlin-1 proteins were clearly observed in many organs, including cerebral cortex, cerebellum, medulla, and spinal cord (Fig. 2E). Since human SOD1^{G93A} gene is driven by human SOD1 promoter, SOD1^{G93A} was widely expressed as expected in SOD1^{G93A} mouse tissues (Fig. 2E; Epstein et al. 1987; Gurney et al. 1994). We also found that expression of SOD1^{G93A} in neuronal tissues and liver was higher than that in other organs and that the interaction of Derlin-1 with SOD1^{mut}, but not SOD1^{wt}, was observed specifically in these tissues (Fig. 2E). The regionally specific interaction of Derlin-1 with SOD1^{mut} might thus be one of the reasons why SOD1^{mut} specifically targets neuronal tissues.

SOD1^{mut} interacts with the C-terminal cytoplasmic region of Derlin-1

Although SOD1^{mut} itself has neither a signal sequence nor transmembrane segment and is located mainly in the cytosol, it has been reported that SOD1^{mut} accumulates in the ER (Kikuchi et al. 2006; Urushitani et al. 2006). We therefore examined whether SOD1^{mut} resides in the ER lumen or associates with the cytosolic side of the ER membrane. Purified microsomal fraction enriched in the ER membrane was isolated from the spinal cord of a SOD1^{G93A} mouse. We found that SOD1^{G93A} exists mainly in the cytosolic fraction and some in the microsomal fraction (Fig. 2F). The alkaline extraction clearly released SOD1^{G93A}, but not Derlin-1, from the microsome, as seen for p97, which is known to be peripherally associated with the ER membrane (Fig. 2F). These findings indicated that SOD1^{mut} exists mainly in the cytosol, and some fraction of SOD1^{mut} attaches to the cytosolic surface of the ER.

Derlin-1 contains a domain named for yeast Der1p (Der1-like domain) and is a protein that spans the ER membrane four times, with both its N and C termini

Nishitoh et al.

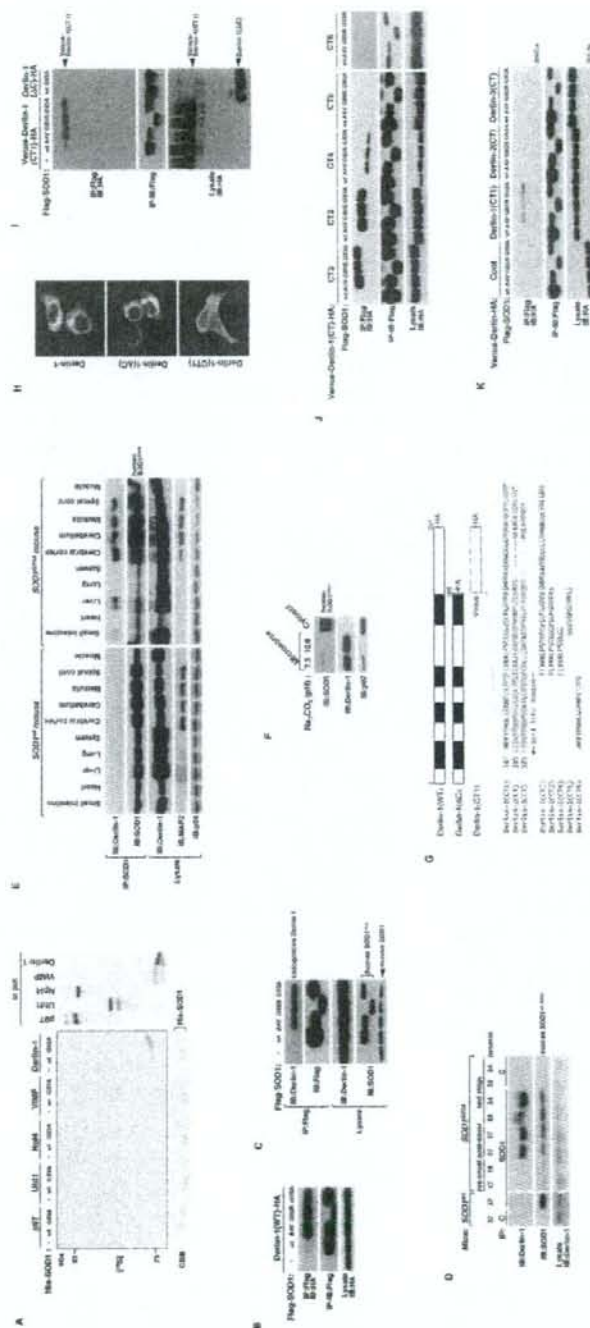


Figure 2. SOD1^{mut} interacts with Derlin-1. (A) ³⁵S-labeled p97, Uf41, Np44, VIMP, or Derlin-1 proteins were incubated with recombinant His-SOD1^{wt} or SOD1^{mut} proteins and immobilized on Ni-NTA beads (top left). The bottom part of the SDS-PAGE gel was stained with Coomassie brilliant blue dye (CBB). Amounts of incubated ³⁵S-labeled proteins are shown (input). (B) Lysates from HEK293 cells, transfected at the indicated combinations, were analyzed by IP-IB. (C) Lysates from HEK293 cells were transfected with Ad-Flag-SOD1^{wt}, Ad-Flag-SOD1^{AV}, Ad-Flag-SOD1^{CSK}, or Ad-Flag-SOD1^{CSMA} for 48 h and analyzed by IP-IB. (D) Extracts from spinal cords of mice were immunoprecipitated with an antibody to SOD1 (IP: SOD1) or control nonimmune antibody (IP: C) and analyzed by IB with antibodies to Derlin-1 and SOD1. The presence of Derlin-1 in the same lysates is shown. (E) Extracts from tissues of SOD1^{wt} mice and SOD1^{mut} mice were analyzed by IB with antibodies to Derlin-1, MAP2, or p88. Interaction between SOD1^{wt} and Derlin-1 in tissues of SOD1^{wt} mice was analyzed by IP-IB. (F) Spinal cord of SOD1^{CSMA} mouse was homogenized and the microsomes were isolated from the post-nuclear and post-mitochondria homogenate. For alkaline extraction, the microsomes were incubated in 100 mM Na₂CO₃ (pH 7.5 or pH 10.9). After the incubation, the microsomes were pelleted and analyzed by IB with antibodies to Derlin-1, SOD1, and p97. Derlin-1 and p97 were used as controls for ER membrane-anchored protein and peripheral protein, respectively. (G) Schematic representation of various mutant forms of Derlin-1. Transmembrane domains of Derlin-1 are shown by black boxes. Identical residues of C-terminal fragment of Derlin family proteins are shaded. (H) HEK293 cells were transfected with various mutant forms of Derlin-1 and stained with antibody to HA. [I-K] Lysates from HEK293 cells, transfected at the indicated combinations, were analyzed by IP-IB.

facing the cytosol (Fig. 2G; Lilley and Ploegh 2004; Ye et al. 2004). To determine the domain of interaction, we constructed expression plasmids for a C-terminally truncated Derlin-1 protein [Derlin-1(Δ C)], which exhibited a reticular pattern, typical of ER localization, and for a C-terminal fragment of Derlin-1 [Derlin-1(CT1)], which exhibited cytosolic localization (Fig. 2H). Derlin-1(CT1), but not Derlin-1(Δ C), coimmunoprecipitated with SOD1^{mut} (Fig. 2I), indicating that SOD1^{mut} associates with the C-terminal cytosolic region of Derlin-1. To further investigate the region of interaction of Derlin-1(CT1) with SOD1^{mut}, various truncation mutants of the C-terminal fragment of Derlin-1 were assessed for interaction with SOD1^{mut}. Derlin-1(CT1), Derlin-1(CT2), Derlin-1(CT3), and Derlin-1(CT4), but not Derlin-1(CT5) and Derlin-1(CT6), were coimmunoprecipitated with SOD1^{mut} (Fig. 2J), indicating that Derlin-1(CT4), composed of 12 amino acids (FLYRWLPSRRGG), is minimally required and sufficient for interaction with SOD1^{mut}. Mammals also express two additional Derlin-like homologs to Derlin-1, designated Derlin-2 and Derlin-3 (Oda et al. 2006). To examine whether SOD1^{mut} also interacts with other Derlin family proteins, C-terminal fragments of Derlin-2 and Derlin-3 [Derlin-2(CT) and Derlin-3(CT), respectively] were assessed for interaction with SOD1^{mut}. Derlin-2(CT) and Derlin-3(CT) were not coimmunoprecipitated with SOD1^{mut} (Fig. 2K), suggesting that, among the Derlin family proteins, SOD1^{mut} associates specifically with Derlin-1. Moreover, since mRNA expression of Derlin-1 was more abundant than that of Derlin-2 and Derlin-3 in brain (Oda et al. 2006), SOD1^{mut} in neuronal tissues probably targets ERAD through specific binding to Derlin-1.

SOD1^{mut} attenuates the retro-translocation of ERAD substrates on the components of ERAD machinery

There are at least three models for the mechanism of how ERAD is inhibited by SOD1^{mut}: (1) Since the C-terminal domain of Derlin-1 has been shown to be necessary for the recruitment of p97 on the ER membrane through binding with VIMP [Ye et al. 2004; Lilley and Ploegh 2005], SOD1^{mut} might inhibit the assembly of Derlin-1, VIMP, and p97 on the ER membrane; (2) since Derlin-1 has been reported to form homo- as well as hetero-oligomers and the ERAD complex with HRD1, an ER-anchored ubiquitin E3 ligase [Lilley and Ploegh 2005; Schulze et al. 2005; Ye et al. 2005; Oda et al. 2006], SOD1^{mut} might inhibit the interaction of Derlin-1 with these ERAD components; (3) SOD1^{mut} might inhibit the directional flow of ERAD substrates at a certain step of their transfer from the ER lumen to p97 or E3 ligase. If the first two models were correct, overexpression of SOD1^{mut} would inhibit the coimmunoprecipitation of Derlin-1 with VIMP, p97, or the other ERAD components. However, we could not detect any dissociation of VIMP (Fig. 3A), p97 (Fig. 3B), Derlin family proteins, and HRD1 (Fig. 3C) from Derlin-1 by SOD1^{mut}. To test model 3, we examined the interaction of an ERAD substrate (NHK) with Derlin-1. SOD1^{mut}, but not SOD1^{wt},

induced the interaction between NHK and Derlin-1 (Fig. 3D, top panel, lanes 2, 6–8). Furthermore, NHK was found to associate with VIMP in the presence of Derlin-1 and SOD1^{mut} (Fig. 3D, second panel, lanes 6–8), suggesting that SOD1^{mut} induces formation of an NHK–Derlin-1–VIMP complex on the ER membrane.

The ERAD substrate that emerged into the cytosol is captured by p97, polyubiquitinated by E3 ligase, and degraded by the proteasome [Tsai et al. 2002; Meusser et al. 2005]. We next examined whether SOD1^{mut} inhibits ubiquitination of NHK. Overexpression of Derlin-1 increased the amount of ubiquitinated NHK in the presence of proteasome inhibitor [MG132] (Fig. 3E, top panel, lane 3), suggesting that Derlin-1 contributes to the degradation of NHK. Expression of SOD1^{mut} clearly decreased the amount of ubiquitinated NHK (Fig. 3E, top panel, lanes 5–7). Furthermore, SOD1^{mut} induced accumulation of nonubiquitinated and deglycosylated NHK in addition to glycosylated NHK (Fig. 3E, second panel, lanes 5–7), suggesting that SOD1^{mut} blocks the presentation of NHK from retro-translocon to E3 ligase. These data also suggested that SOD1^{mut} does not inhibit the assembly of essential components of retro-translocon per se but does trap ERAD substrates on the complex composed of SOD1^{mut}–Derlin-1–VIMP and thereby inhibits subsequent transfer of ERAD substrates to the ubiquitination step by E3.

SOD1^{mut} activates the IRE1–TRAF2–ASK1 pathway

It has been reported that the ASK1–p38 pathway is activated in motor neurons of the spinal cord of SOD1^{G93A} mice [Wengenack et al. 2004; Holasek et al. 2005; Veglianesi et al. 2006]. To investigate the role of ASK1 in the motor neurotoxicity by SOD1^{mut}, we examined whether SOD1^{mut} activates ASK1 as assessed by *in vitro* kinase assay. Expression of SOD1^{mut}, but not SOD1^{wt}, activated endogenous ASK1 (Fig. 4A, top panel). We next examined whether SOD1^{mut}-induced ASK1 activation is mediated by ER stress. Activated IRE1 has been demonstrated to recruit TRAF2 and ASK1 on the ER membrane and thus to activate ASK1 [Nishitoh et al. 2002]. We examined whether SOD1^{mut} induces interaction between endogenous ASK1 and TRAF2. ASK1 was found to associate with TRAF2 in NSC34 cells infected with Ad-SOD1^{mut} but not those infected with Ad-SOD1^{wt} (Fig. 4A, third panel). To further examine whether IRE1 recruits TRAF2 and ASK1 in SOD1^{mut}-expressing cells, Ad-SOD1, Ad-ASK1, Ad-IRE1, and Lentivirus encoding [Len]-TRAF2 were infected into NSC34 cells and subjected to coimmunoprecipitation analysis. ASK1 was found to associate with IRE1 only in the presence of TRAF2 and SOD1^{mut} (Fig. 4B), suggesting that SOD1^{mut} induces formation of an IRE1–TRAF2–ASK1 complex on the ER membrane and thus activates ASK1 by triggering ER stress-induced IRE1 activation.

We next assessed the requirement of Derlin-1 for SOD1^{mut}-induced ER stress and ASK1 activation using siRNA against Derlin-1. Derlin-1 siRNA effectively sup-

Nishitoh et al.

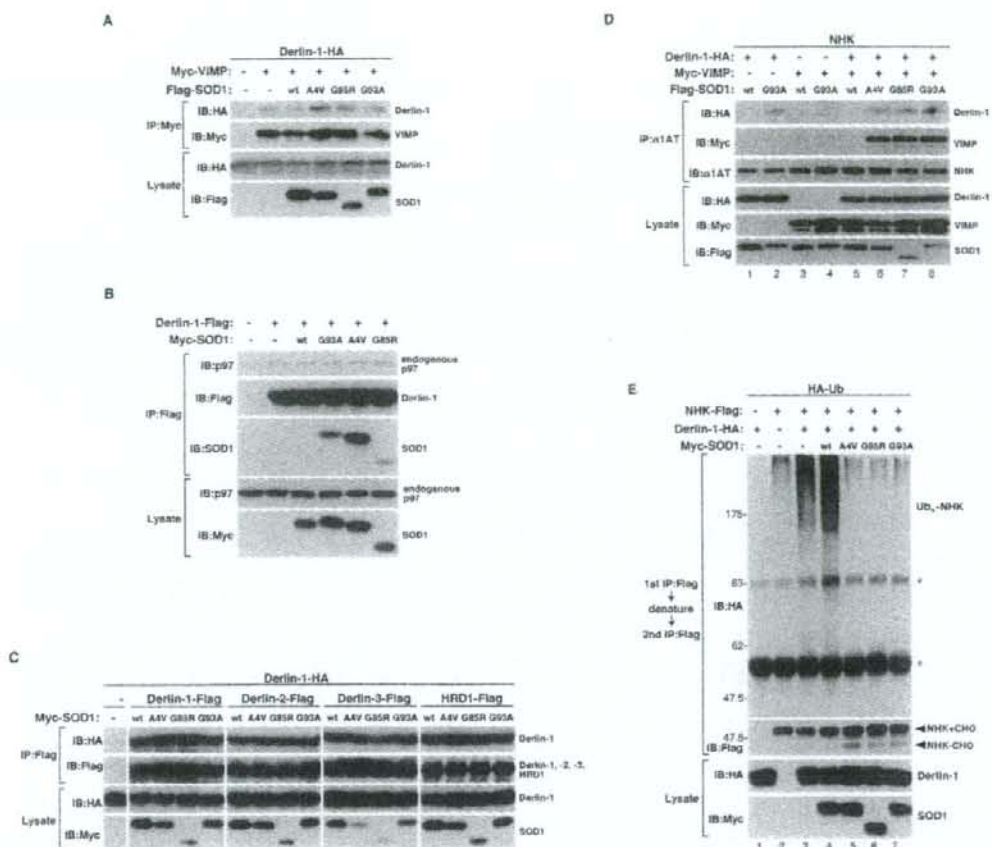


Figure 3. SOD1^{mut} attenuates the retro-translocation of ERAD substrate on the components of ERAD. (A) Lysates from HEK293 cells, transfected with Derlin-1-HA, Myc-VIMP, and Flag-SOD1 at the indicated combinations, were analyzed by IP-IB. The presence of Derlin-1-HA and Flag-SOD1 in the same lysates is shown. (B) Lysates from HEK293 cells, transfected at the indicated combinations, were analyzed by IP-IB. The presence of p97 and Myc-SOD1 in the same lysates is shown. (C) Lysates from HEK293 cells, transfected at the indicated combinations, were analyzed by IP-IB. The presence of Derlin-1-HA and Myc-SOD1 in the same lysates is shown. (D) Lysates from HEK293 cells, transfected with NHK, Derlin-1-HA, Myc-VIMP, and Flag-SOD1 at the indicated combinations, were analyzed by IP-IB. The presence of Derlin-1-HA, Myc-VIMP, and Flag-SOD1 in the same lysates is shown. (E) HEK293 cells were transfected with NHK-Flag, Derlin-1-HA, Myc-SOD1, and HA-Ub at the indicated combinations and incubated with 0.25 μ M MG132 for 18 h. NHK was immunoprecipitated with antibody to Flag. After incubation with the denaturing buffer containing 1% SDS, NHK was reimmunoprecipitated with antibody to Flag. Samples were immunoblotted with antibodies to HA and Flag. The presence of Derlin-1-HA and Myc-SOD1 in the same lysates is shown. Asterisks denote nonspecific bands and IgG.

pressed expression of Derlin-1 without affecting that of Derlin-2, ASK1, p38, or TRAF2 (Fig. 4C,E). We examined whether reducing Derlin-1 expression levels affected the ER stress response using band-shift analyses of IRE1 and Xbp-1 mRNA splicing, which is caused by the activated RNase domain of IRE1. Derlin-1 siRNA exhibited no effect on the basal level of activation of IRE1 (Fig. 4C [lanes 1,5], D [lanes 1,7,13]) and thapsigargin-induced activation of IRE1 (Fig. 4C [lanes 4,8], D [lanes 6,12,18]), suggesting that Derlin-1 is not essential for ERAD in NSC34

cells. Interestingly, however, SOD1^{mut}-induced activation of IRE1 and ASK1 was clearly inhibited by Derlin-1 depletion (Fig. 4C [lane 7], D [lanes 9–11,15–17]). Furthermore, SOD1^{mut}-induced interaction between TRAF2 and ASK1 was inhibited by Derlin-1 depletion (Fig. 4E, lanes 9–11,15–17), suggesting that Derlin-1 is selectively required for the SOD1^{mut}-induced ER stress. These results also suggested that SOD1^{mut} induces ERAD dysfunction not by a simple loss of function but by a gain of malfunction of Derlin-1.

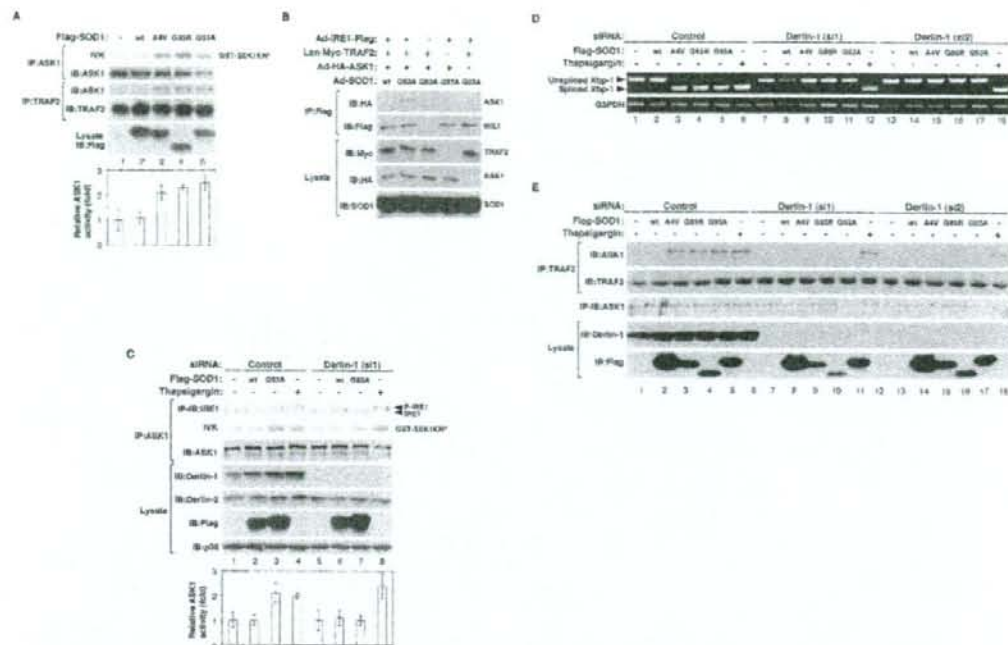


Figure 4. SOD1^{mut} activates the IRE1-TRAF2-ASK1 pathway. (A) NCS34 cells were infected with Ad-SOD1^{wt}, Ad-SOD1^{Δ4V}, Ad-SOD1^{G85R}, or Ad-SOD1^{G93A} for 48 h. ASK1 activity was measured by *in vitro* kinase assay (IVK). (GST-SEK1KN)^{ph} Phosphorylated GST-SEK1KN. Interaction between TRAF2 and ASK1 was analyzed by IP with antibody to TRAF2 and IB with antibody to ASK1. The presence of ASK1, TRAF2, and SOD1 in the same lysates is shown. (Lane 1) Kinase activity relative to the amount of ASK1 protein is shown as fold increase compared with control cells. (B) NCS34 cells were infected with adenoviruses and lentivirus at the indicated combinations. SOD1^{mut}-dependent IRE1-TRAF2-ASK1 complex formation were analyzed by IP-IB. (C) NCS34 cells, transfected with siRNA against Derlin-1 (si1) or nonspecific sequence (Control), were infected with Ad-SOD1^{wt} or Ad-SOD1^{G93A} for 48 h or treatment with 10 μM Thapsigargin for 2 h. Activation of IRE1 and ASK1 was analyzed by IP-IB with antibodies to IRE1α and by IVK using GST-SEK1KN as a substrate, respectively. The presence of ASK1, Derlin-1, Derlin-2, SOD1, and p38 in the same lysates is shown. (Lanes 1,5) Kinase activity relative to the amount of ASK1 protein is shown as fold increase compared with control cells. (D,E) NCS34 cells, transfected with siRNA against Derlin-1 (si1), Derlin-1 (si2), or nonspecific sequence (Control), were infected with Ad-SOD1^{wt}, Ad-SOD1^{Δ4V}, Ad-SOD1^{G85R}, or Ad-SOD1^{G93A} for 48 h or treatment with 2 μM thapsigargin for 2 h. Xbp-1 mRNA splicing was determined by RT-PCR. Interaction between TRAF2 and ASK1 was analyzed by IP with antibody to TRAF2 and IB with antibody to ASK1. The presence of TRAF2, ASK1, Derlin-1, and Flag-SOD1 in the same lysates is shown.

Dissociation of SOD1^{mut} from Derlin-1 protects motor neurons from SOD1^{mut}-induced cell death

Based on the above findings, which indicate that SOD1^{mut} proteins induce ER stress by interacting with Derlin-1, we hypothesized that forced dissociation of SOD1^{mut} from Derlin-1 may restore normal function of ERAD and thus suppress SOD1^{mut}-induced motor neurotoxicity. We examined the effect of Derlin-1(CT4) on the interaction between SOD1^{mut} and Derlin-1. When Derlin-1(CT4) but not control (Venus-HA) or Derlin-1(CT5) was coexpressed, binding of Derlin-1 to SOD1^{mut} was strongly inhibited (Fig. 5A). Reciprocally, Derlin-1(CT4) was found to associate with SOD1^{mut} in a dose-dependent fashion (Fig. 5A). We next examined the effect of Derlin-1(CT4) on SOD1^{mut}-induced ER stress and ASK1 activation. Derlin-1(CT4) inhibited SOD1^{mut}-in-

duced activation of IRE1, PERK, and ASK1 (Fig. 5B). These findings suggested that the interaction between SOD1^{mut} and Derlin-1 plays a central role in the activation of the ER stress-ASK1 pathway.

We next investigated the effects of Derlin-1(CT4) on SOD1^{mut}-induced cell death using spinal cord cultures derived from E12.5 mouse embryos (Urushitani et al. 2006). At 7 d after plating, spinal cord cultures were infected with Len-SOD1^{wt} or Len-SOD1^{mut} with Len-Derlin-1(CT4) or control (Venus-HA) lentivirus for additional 3 d. Expression of neither SOD1^{wt} nor SOD1^{G93A} affected the number of glial cells (Fig. 5C,F). In contrast, the number of motor neurons that were stained with antibody to unphosphorylated neurofilament-H (SMI32) was strongly decreased by SOD1^{G93A} (Fig. 5C,E) and SOD1^{G85R} (Supplemental Fig. S5A,B), indicating that SOD1^{mut} was selectively toxic to motor neurons and not

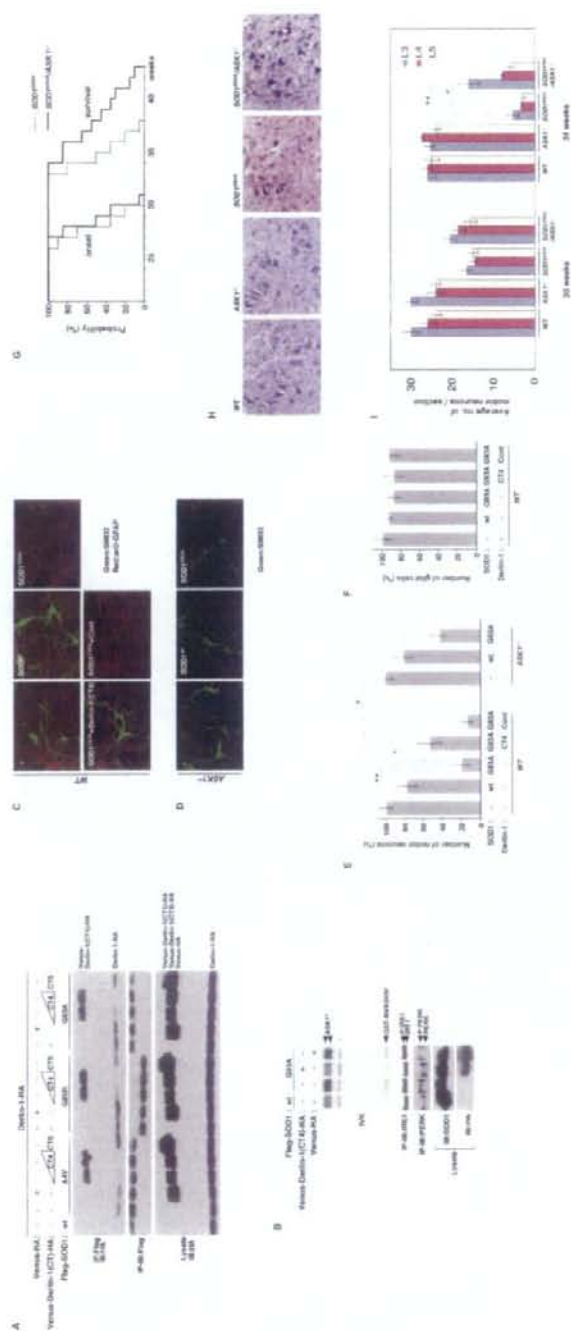


Figure 5. Impairment of SOD1^{mut}-Derlin-1 interaction and deletion of ASK1 mitigate SOD1^{mut}-induced motor neurotoxicity. (A) Lysates from HEK293 cells, transfected at the indicated combinations, were analyzed by IP-IB. (B) NSC34 cells were infected with Ad-SOD1^{G93A}, Len-Venus-Derlin-1 (CT4)-HA, and Len-Venus-HA at the indicated combinations for 48 h. Activation of IRE1 and PERK was examined as described in Figure 1A. Activation of ASK1 was analyzed by IVK using GST-MKK6KN as substrate. [ASK1]^Δ Autophosphorylated ASK1. [GST-MKK6KN]^Δ Phosphorylated GST-MKK6KN. Asterisk denotes nonspecific bands. (C) Wild-type mice spinal cord cultures were infected with lentivirus at the indicated combinations for 72 h. Cultures were fixed and doubly stained with antibodies to nonphosphorylated neurofilament (SMI32) (green) and GFAP (red). (D) ASK1^{-/-} mice spinal cord cultures were infected as indicated and stained with SMI32 antibody. (E) The percentage of total cell count of SMI32 antibody-positive cells is shown compared with control culture (wild type; $n = 3$); [ASK1^{-/-}; $n = 5$]. Values are means \pm SE of independent experiments. (* $P < 0.05$; (** $P < 0.01$), significance calculated by Student's t -test. (# $P < 0.05$ significance calculated by ANOVA. (F) The percentage of total cell count of anti-GFAP antibody-positive cells derived from wild-type mice is shown compared with control culture. Values are means \pm SE of three independent experiments. (G) The onset of disease was determined by motor function deficit seen in rota-rod performance in SOD1^{G93A} mice in the presence or absence [ASK1^{-/-}] of ASK1. The cumulative probability of onset of rota-rod deficit was not significantly changed in SOD1^{G93A}/ASK1^{-/-} mice ($n = 10$; solid line) compared with SOD1^{G93A} mice ($n = 10$; dotted line). Probabilities of survival reveal prolongation of life span of SOD1^{G93A}/ASK1^{-/-} mice ($n = 20$; solid line) compared with SOD1^{G93A} mice ($n = 20$; dotted line). The data were analyzed by the Kaplan-Meier life test and by long-rank test. (H) Cresyl violet (Nissl)-stained paraffin sections of ventral horn from lumbar (level L3) spinal cords at end stage (age 34 wk) are shown. (I) Stereological analysis of motor neuron death. Numbers of motor neurons were determined by counting the large Nissl-positive neurons in the ventral horn. Five mice of each group were used for analysis. Thirty-week-old and 34-wk-old mice were sacrificed, and sections of lumbar spinal cord at levels L3, L4, and L5 were counted for each mouse. Values are means \pm SE. (* $P < 0.05$; (** $P < 0.01$), significance calculated by Student's t -test.

glial cells. SOD1^{mut}-induced motor neuron death was significantly attenuated by coexpression of Derlin-1[CT4] (Fig. 5C,E; Supplemental Fig. S5A,B). These findings are consistent with the inhibitory effects of Derlin-1[CT4] on the binding between SOD1^{mut} and Derlin-1 and on the ER stress-mediated activation of ASK1, and thus strongly suggested that induction of dysfunction of Derlin-1 by SOD1^{mut} may contribute to the pathogenesis of familial ALS.

ASK1 deficiency mitigates motor neuron death and prolongs survival of ALS mice

Finally, we examined the requirement of ASK1 for SOD1^{mut}-induced motor neuron death. Spinal cord cultures derived from wild-type and *ASK1*^{-/-} mice were infected with Len-SOD1^{wt} or Len-SOD1^{G93A}. ASK1 deficiency did not affect the expression of SOD1^{wt} or SOD1^{G93A} (Supplemental Fig. S6). *ASK1*^{-/-} neurons were significantly more resistant to SOD1^{mut}-induced cell death than were wild-type neurons (Fig. 5D,E). Inhibition of SOD1^{mut}-induced cell death in *ASK1*^{-/-} neurons was not significantly enhanced by the expression of Derlin-1[CT4] (Supplemental Fig. S7), suggesting that the ASK1-dependent signal may serve as a major cell death pathway in the downstream SOD1^{mut}-induced ER stress. To further evaluate the role of ASK1 in the pathogenesis of ALS *in vivo*, we tested whether ASK1 deficiency ameliorates the motor neuropathological alterations in ALS mice. We produced *SOD1*^{G93A} mice that lacked *ASK1* (*SOD1*^{G93A}/*ASK1*^{-/-} mice) (Supplemental Fig. S8B) and compared their time of disease onset and life span with those of *SOD1*^{G93A} mice. Time of disease onset was determined as that of loss of motor function. On rota-rod testing, no significant difference was found between *SOD1*^{G93A} and *SOD1*^{G93A}/*ASK1*^{-/-} mice (Fig. 5G). However, the mean survival of *SOD1*^{G93A}/*ASK1*^{-/-} mice was 38.4 ± 2.7 wk (\pm SEM) and significantly longer than the 34.9 ± 1.6 wk survival of control *SOD1*^{G93A} mice (long rank = 17.0206, $P < 0.0001$) (Fig. 5G). We also examined the time of disease onset and life span using *SOD1*^{G93A} high copy [*SOD1*^{G93A}(*high*)] mice. ASK1 deficiency also extended the survival of *SOD1*^{G93A}(*high*) mice but not the time of onset (Supplemental Fig. S9). These findings indicated that ASK1 deficiency extends the survival of ALS mice by ameliorating disease progression. To assess the role of ASK1 in spinal motor neuron death *in vivo*, we examined L3, L4, and L5 spinal sections from wild-type, *ASK1*^{-/-}, *SOD1*^{G93A}, and *SOD1*^{G93A}/*ASK1*^{-/-} mice. At the end stage, *SOD1*^{G93A} mice exhibited fewer motor neurons in the anterior horn of the spinal cord than age-matched wild-type or *ASK1*^{-/-} mice (Fig. 5H; Supplemental Fig. S10A). In contrast, a larger number of motor neurons were significantly found in the upper (L3 and L4) spinal cord from *SOD1*^{G93A}/*ASK1*^{-/-} than in that from *SOD1*^{G93A} mice (Fig. 5H,I; Supplemental Fig. S10A,B). These findings indicated that the absence of ASK1 mitigates motor neuron death in ALS mice.

Discussion

A novel pathogenic mechanism of SOD1^{mut}-mediated ALS is supported by the findings that SOD1^{mut} interacts specifically with Derlin-1 and that this interaction impairs ERAD and leads to ER stress-dependent activation of ASK1 (Fig. 6). The nearly complete loss of SOD1^{mut}-induced ER stress and activation of ASK1 by reduced expression of Derlin-1 or by overexpression of Derlin-1[CT4] strongly suggests that the binding between SOD1^{mut} and Derlin-1 is an important step in the SOD1^{mut}-induced ER stress signaling pathway. It has been reported that translocon-associated protein (TRAP) δ interacts with SOD1^{mut} (Kunst et al. 1997) and that TRAP complex including TRAP δ is required for ERAD (Nagasawa et al. 2007), suggesting that the association of SOD1^{mut} with TRAP δ may also be involved in SOD1^{mut}-induced ER stress.

It is unclear how various SOD1^{mut} proteins interact with Derlin-1. SOD1^{L126Z}, a simple C-terminal deletion mutant (Supplemental Fig. S11A), which causes motor neuron disease in mice (Wang et al. 2005), also interacted with Derlin-1 (Supplemental Fig. S11B). Therefore, the Derlin-1 interaction domain of SOD1^{wt} might be concealed by proper folding and be bared by mutation-dependent unfolding of SOD1^{mut}. Another hypothesis is that chaperon proteins might mediate the interaction between SOD1^{mut} and Derlin-1. Although the results from our *in vitro* studies using recombinant SOD1 proteins

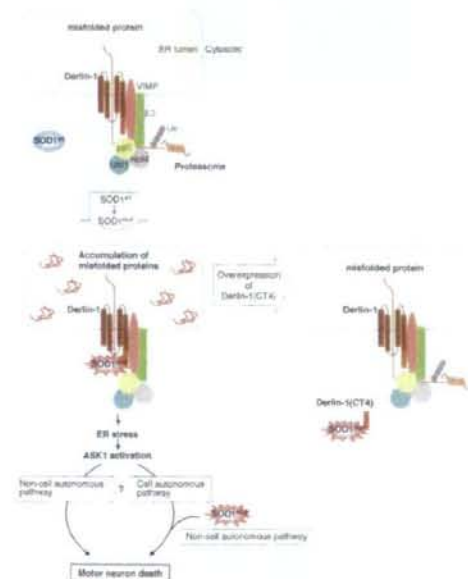


Figure 6. Schematic representation of the mechanism of SOD1^{mut}-induced motor neuron death through ER stress. See the text for details.

Nishitoh et al.

support a direct interaction between SOD1^{mut} and Derlin-1 (Fig. 2A), we cannot rule out the possibility that chaperon proteins in the reticulocyte lysate mediate the interaction between SOD1^{mut} and Derlin-1. SOD1^{mut}, but not SOD1^{wt}, is known to interact with heat shock proteins, including Hsp25 and Hsp/Hsc70 (Shinder et al. 2001; Wang et al. 2003; Urushitani et al. 2004).

It is still unclear how the association of SOD1^{mut} with Derlin-1 inhibits the ERAD pathway. Derlin-1 is one of the components required for retro-translocation of misfolded proteins from the ER lumen to the cytoplasm (Lilley and Ploegh 2004; Ye et al. 2004). Derlin-1-mediated retro-translocation is currently believed to occur as follows (Meusser et al. 2005): (1) The substrate is recognized by ER chaperones or ER membrane receptors and is targeted to a retro-translocon; (2) Derlin-1 recruits a membrane complex containing VIMP, the p97 complex, and an E3 ligase; (3) once the substrate emerges into the cytosol, it is captured by p97 as a result of its AAA-ATPase activity and polyubiquitinated by E3; and (4) subsequently, the polyubiquitinated substrates are degraded by the proteasome. The present finding that inhibition of proteasomal activity was undetectable by SOD1^{mut} at the time at which SOD1^{mut}-induced ER stress was evoked (Fig. 1D; Supplemental Fig. S2A) suggests that it is unlikely that SOD1^{mut} primarily targeted final step 4. If SOD1^{mut} disturbs the initiation step 1 of retro-translocation, SOD1^{mut} may inhibit interaction between the unfolded substrate and Derlin-1. However, binding between NHK and Derlin-1 was clearly observed even in SOD1^{mut}-overexpressing cells (Fig. 3D). Moreover, SOD1^{mut} did not inhibit association of Derlin-1 with VIMP, p97, Derlin family proteins, and HRD1 (Fig. 3A-C), suggesting that SOD1^{mut} may not perturb step 2. However, we cannot rule out the possibility that SOD1^{mut} inhibits additional interactions between Derlin-1 and its partners in the ERAD complex. Since ubiquitination of ERAD substrate was inhibited by SOD1^{mut} (Fig. 3E), SOD1^{mut} may thus disturb the presentation of ERAD substrate to the p97 complex or E3. Although exactly how SOD1^{mut} inhibits the directional flow of ERAD substrates remains to be elucidated, it is imaginable that ERAD substrates trapped on the SOD1^{mut}-Derlin-1-VIMP complex would interfere with further disposal of de novo ERAD substrates like a traffic jam, eventually leading to the accumulation of misfolded proteins within the ER lumen.

Although the prolongation of survival of SOD1^{G93A}/ASK1^{-/-} mice clearly indicated the requirement of ASK1 for disease progression, ASK1 deficiency was not sufficient to attenuate disease onset (Fig. 5G; Supplemental Fig. S9). These findings are supported by a recent study that demonstrated the contribution of caspase-9 to motor neuron death and disease progression but not to disease onset in *X-chromosome-linked inhibitor of apoptosis* (*XIAP*; a mammalian inhibitor of caspase-3 and caspase-9) transgenic mice (Inoue et al. 2003). We reported previously that ASK1-induced apoptosis is dependent on caspase-9 activation (Hatai et al. 2000), suggest-

ing that the ASK1-caspase-9 proapoptotic pathway may be crucial only for disease progression. On the other hand, several groups have reported that the p38, but not JNK, pathway is activated in motor neurons of the spinal cord of SOD1^{G93A} mice (Wengenack et al. 2004; Holasek et al. 2005; Veglianese et al. 2006). Thus, the ASK1-p38 and/or ASK1-caspase-9 pathway may specifically contribute to SOD1^{mut}-induced motor neuron death.

Since expression of Derlin-1(CT4) and deletion of ASK1 only partially mitigated SOD1^{mut}-induced motor neuron death in vitro (Fig. 5E; Supplemental Fig. S5B), the ER stress-ASK1 pathway-independent cell death mechanism including proteasomal dysfunction (Urushitani et al. 2002; Puttapparthi et al. 2003) may also exist in the pathogenesis of ALS. This may reflect, in part, the incomplete resistance of motor neuron death by ASK1 deficiency in ALS mice (Fig. 5I; Supplemental Fig. S10B). Furthermore, the effect of loss of ASK1 on cell death was slightly weaker than that of Derlin-1(CT4) (Fig. 5E), and Derlin-1(CT4) slightly, although not significantly, enhanced the inhibition of SOD1^{mut}-induced cell death in ASK1^{-/-} neurons (Supplemental Fig. S7). These results suggest that other ER stress-induced proapoptotic pathways, including PERK (Jordan et al. 2002) and CHOP (Zinszner et al. 1998), might also be involved in the downstream SOD1^{mut}-dependent motor neuron death.

Another important issue to be elucidated is the relationship between the ER stress-mediated signaling pathway and the non-cell-autonomous mechanisms of SOD1^{mut}-induced neurotoxicity. Recent studies have emphasized the importance of non-cell-autonomous mechanisms (Clement et al. 2003; Boillee et al. 2006; Yamanaka et al. 2008). Consistent with their findings, SOD1^{mut} induced motor neuron death in spinal cord cultures (Fig. 5C,E; Supplemental Fig. S5A,B) but not in NSC34 cells (data not shown) in which ER stress-mediated ASK1 activation was clearly observed. However, since expression of SOD1^{mut} in neurons alone (Prattarova et al. 2001) or glial cells alone (Gong et al. 2000) does not induce motor neuron disease in mice, not only non-cell-autonomous mechanisms but also cell-autonomous mechanisms must play roles in SOD1^{mut}-induced neurotoxicity. It is likely that the non-cell-autonomous signals that are transferred from astrocytes, glial cells, or feeder cells to motor neurons are coordinated with and crucial for the ER stress/ASK1-dependent cell-autonomous death signaling induced by SOD1^{mut} (Fig. 6). It is also possible that the ER stress-induced ASK1 activation itself serves as the non-cell-autonomous death signaling (Fig. 6).

In conclusion, our findings demonstrated a novel mechanism by which SOD1^{mut} causes motor neuron death through interaction with Derlin-1, ERAD dysfunction, ER stress, and ASK1 activation. Although further investigation is needed to clarify the mechanisms by which SOD1^{mut} induces the malfunction of Derlin-1 and to identify the downstream effectors of ASK1, Derlin-1 and ASK1 may be potential targets in the treatment of ALS.

Materials and methods

Band-shift analysis for IRE1 and PERK

NSC34 cells were lysed in the lysis buffer as described [Nishitoh et al. 2002]. Cell extracts were clarified by centrifugation, and the supernatants were immunoprecipitated with antibodies to IRE1 α and PERK. Proteins were resolved by SDS-PAGE under reducing conditions and immunoblotted with antibodies to IRE1 α and PERK.

RT-PCR

Total RNA was isolated from 6×10^6 NSC34 cells using ISOGEN kit (Nippongene). Ten micrograms of RNA were reverse-transcribed with SuperScript II (Life Technologies) according to the manufacturer's instructions. The primers used for PCR were as follows: mouse Bip, 5'-AAGGCTCTATGAAGGTGAACGAC CCC-3' and 5'-GACCCCAAGACATGTGAGCAACTGC-3'; mouse Chop, 5'-ACTACTCTTGACCTGCGTCCCTAG-3' and 5'-CATGTGCAGTGCAGTGCAGGGTCCAC-3'; mouse Xbp-1, 5'-GAACCAGGAGTTAAGAACAGC-3' and 5'-AGGCAACA GTGTCAGAGTCC-3'; and mouse G3PDH, 5'-ATGGTGAAG GTCGGTGTAA-3' and 5'-ACATGGCTCCAAGGAGTAA-3'.

Pulse-chase assay

NSC cells were labeled with 35 S-Promix (GE Healthcare) in medium lacking methionine and cysteine for 30 min, and chased in medium containing excess methionine and cysteine. Cells were lysed in a buffer containing 1% NP-40, 150 mM NaCl, 50 mM Tris-HCl (pH 8.0), and protease inhibitor cocktail. An antibody to α 1AT was used for immunoprecipitation. Immunoprecipitated samples were resolved by SDS-PAGE and analyzed by an image analyzer.

In vitro binding assay

His⁶-SOD1^{WT} and His⁶-SOD1^{G93A} were constructed in pTrcHis vector (Invitrogen). Recombinant His-SOD1^{WT} and His-SOD1^{G93A} proteins were purified with Ni-NTA (Qiagen) according to the manufacturer's instructions. In vitro translated 35 S-labeled VCP, Ufd1, Npl4, VIMP, and Derlin-1 were prepared with the TNT Reticulocyte Lysate System (Promega). 35 S-labeled proteins were incubated for 16 h at 4°C with each His-SOD1^{WT} or His-SOD1^{G93A} in buffer containing 150 mM NaCl, 20 mM Tris-HCl (pH 7.5), and 0.5 mM Triton X-100; washed twice with the washing buffer containing 150 mM NaCl, 20 mM Tris-HCl (pH 7.5), 0.5% Triton X-100, and 20 mM Imidazole, and analyzed by SDS-PAGE with an image analyzer.

In vivo binding assay

Binding assay using transfected HEK293 cells has been described [Nishitoh et al. 2002]. For binding assay between over-expressed Flag-SOD1 and endogenous Derlin-1, 5×10^6 NSC34 cells infected with Ad-SOD1^{WT}, Ad-SOD1^{Δ4V}, Ad-SOD1^{G36R}, or Ad-SOD1^{G93A} for 48 h were immunoprecipitated with an antibody to Flag. For endogenous binding assay between SOD1 and Derlin-1, lysates from tissues of SOD1^{WT} or SOD1^{G93A} mice were immunoprecipitated with an antibody to SOD1 or control nonimmune rabbit polyclonal antibody. For endogenous binding assay between TRAF2 and ASK1, lysates from 3×10^7 NSC34 cells were immunoprecipitated with an antibody to

TRAF2 or control nonimmune rabbit polyclonal antibody. Proteins were resolved by SDS-PAGE and immunoblotted with antibodies to Derlin-1, SOD1, ASK1, or TRAF2. Aliquots of the same lysates were subjected to immunoblotting with antibodies to Derlin-1 or Flag. For the complex formation assay of IRE1-TRAF2-ASK1, 1×10^7 NSC34 cells were infected with adenoviruses and lentivirus for 48 h, and lysates were analyzed by immunoprecipitation-immunoblot (IP-IB) as described [Nishitoh et al. 2002].

Subcellular fractionation

A 30-wk-old mouse spinal cord was washed with PBS at 4°C and placed in ice-cold homogenization buffer (10 mM Tris-HCl at pH 7.4, 1 mM EDTA, protease inhibitors). Tissue was homogenized with 40 strokes of a glass-pestle homogenizer on ice. Homogenates were centrifuged at 14,000g for 7 min. Supernatant was centrifuged at 100,000g for 1 h to yield a microsomal pellet. Microsomes were incubated with homogenization buffer containing 100 mM Na₂CO₃ (pH 7.5 or pH 10.9) for 5 min, pelleted by centrifugation at 100,000g for 30 min, and analyzed by IB with an antibody to SOD1, Derlin-1, or p97.

In vitro kinase assay

In vitro kinase assay has been described [Nishitoh et al. 2002]. In brief, infected 1×10^7 NSC34 cells were lysed with the lysis buffer and immunoprecipitated with an antibody to ASK1. Kinase activity of ASK1 was measured using [γ - 32 P]ATP and GST-MKK6KN or GST-SEK1KN as substrate and analyzed by SDS-PAGE with an image analyzer.

Ubiquitination assay

Lysates from transfected HEK293 cells were immunoprecipitated with antibody to Flag. After washing with the washing buffer containing 150 mM NaCl, 20 mM Tris-HCl (pH 7.5), and 5 mM EGTA, beads were boiled with the denaturing buffer containing 1% SDS, 150 mM NaCl, 20 mM Tris-HCl (pH 7.5), and 5 mM EGTA. The supernatant was diluted and reimmunoprecipitated with antibody to Flag and analyzed by SDS-PAGE.

siRNA knockdown of Derlin-1

NSC34 cells were transfected with Derlin-1-specific RNAi oligo and control RNAi oligo (Invitrogen) using Lipofectamine RNAiMAX reagent (Invitrogen). After 24 h, cells were infected with adenovirus for 48 h. Knockdown was analyzed by IB with antibody to Derlin-1. Sequences were as follows: Derlin-1-MSS228692 [si1] Stealth Select RNAi, AUUAGUUGAAUC CAAGGAUAACCC and GGGUUUCCUUGGAUUCAACU AUU; Derlin-1-MSS228693 [si2] Stealth Select RNAi, AGUAA CAGGCCUUAAAUCGCGUCC and GGAACGCGAUUUAA GGGCCUUUACU; and Stealth RNAi Negative Control Medium GC Duplex.

Motor neuron death assay

Spinal cords [Urushitani et al. 2002] were subjected to primary culture for 7 d and infected with lentivirus for 72 h. Cells were stained with antibody to GFAP (1:100; DAKO) and SMI32 antibody (1:1000; Covance).

Nishitoh et al.

Mice

Both *SOD1^{G93A}* transgenic mice [G1L/+ line, backcrossed to C57BL/6 mice; Jackson Laboratories], which expressed human *SOD1^{G93A}* gene, and *SOD1^{WT}* transgenic mice, which expressed >8 copies of human *SOD1^{WT}* gene, were used. An *ASK1^{-/-}* mouse [Tobiume et al. 2001] was mated with a *SOD1^{G93A}* mouse under pathogen-free conditions. To circumvent potential difficulties caused by sex of mice, male mice were utilized in the present study. The onset of disease was determined by motor function deficit seen in rota-rod performance at an accelerated speed to 40 rpm for 5 min. All mouse experiments accorded with protocols approved by the Animal Research Committees of Tokyo Medical and Dental University and the University of Tokyo.

Nissl staining

Mice were perfused with PBS followed by 4% PFA in PBS. The spinal cords were excised, fixed with 4% PFA in PBS for 1 d, embedded in paraffin, and sectioned (4 μ m). After being deparaffinized using standard protocols, paraffin sections were nissl-stained with cresyl violet. All motor neuron counts were performed in a blinded fashion. We counted the numbers of motor neurons in every fifth section of L3, L4, and L5. Only the large-size neurons with a clear nucleolus and distinctly labeled cytoplasm were included in cell counts.

Acknowledgments

We thank R. Takahashi and M. Urushitani for kind instruction for the primary motor neuron culture; D. Ron, F. Urano, T.A. Rapoport, and Y. Ye for providing antibodies; K. Nagata and N. Hosokawa for providing NHK plasmid, and D. Trono for providing the lentiviral vector system. We also thank all the members of Cell Signaling Laboratory for their critical comments. This study was supported by Grant-in-Aid for Scientific Research on Priority Areas, Research on Pathomechanisms of Brain Disorders, from the Ministry of Education, Culture, Sports, Science and Technology of Japan, CREST, Japan Science and Technology Corporation, Takeda Science Foundation, and The Nakabayashi Trust for ALS Research.

References

- Atkin, J.D., Farg, M.A., Turner, B.J., Tomas, D., Lysaght, J.A., Nunan, J., Rembach, A., Nagley, P., Beart, P.M., Cheema, S.S., et al. 2006. Induction of the unfolded protein response in familial amyotrophic lateral sclerosis and association of protein disulfide isomerase with superoxide dismutase 1. *J. Biol. Chem.* **281**: 30152–30165.
- Boillee, S., Yamanaka, K., Lobsiger, C.S., Copeland, N.G., Jenkins, N.A., Kassiotis, G., Kollias, G., and Cleveland, D.W. 2006. Onset and progression in inherited ALS determined by motor neurons and microglia. *Science* **312**: 1389–1392.
- Bowling, A.C., Schulz, J.B., Brown Jr., R.H., and Beal, M.F. 1993. Superoxide dismutase activity, oxidative damage, and mitochondrial energy metabolism in familial and sporadic amyotrophic lateral sclerosis. *J. Neurochem.* **61**: 2322–2325.
- Clement, A.M., Nguyen, M.D., Roberts, E.A., Garcia, M.L., Boillee, S., Rule, M., McMahon, A.P., Doucette, W., Siwek, D., Ferrante, R.J., et al. 2003. Wild-type nonneuronal cells extend survival of *SOD1* mutant motor neurons in ALS mice. *Science* **302**: 113–117.
- Epstein, C.J., Avraham, K.B., Lovett, M., Smith, S., Elroy-Stein, O., Rotman, G., Bry, C., and Groner, Y. 1987. Transgenic mice with increased Cu/Zn-superoxide dismutase activity: Animal model of dosage effects in Down syndrome. *Proc. Natl. Acad. Sci.* **84**: 8044–8048.
- Fang, S., Ferrone, M., Yang, C., Jensen, J.P., Tiwari, S., and Weissman, A.M. 2001. The tumor autocrine motility factor receptor, gp78, is a ubiquitin protein ligase implicated in degradation from the endoplasmic reticulum. *Proc. Natl. Acad. Sci.* **98**: 14422–14427.
- Gong, Y.H., Parsadanian, A.S., Andreeva, A., Snider, W.D., and Elliott, J.L. 2000. Restricted expression of G86R Cu/Zn superoxide dismutase in astrocytes results in astrocytosis but does not cause motoneuron degeneration. *J. Neurosci.* **20**: 660–665.
- Gurney, M.E., Pu, H., Chiu, A.Y., Dal Canto, M.C., Polchow, C.Y., Alexander, D.D., Caliendo, J., Hentati, A., Kwon, Y.W., Deng, H.X., et al. 1994. Motor neuron degeneration in mice that express a human Cu,Zn superoxide dismutase mutation. *Science* **264**: 1772–1775.
- Hatai, T., Matsuzawa, A., Inoshita, S., Mochida, Y., Kuroda, T., Sakamaki, K., Kuida, K., Yonehara, S., Ichijo, H., and Takeda, K. 2000. Execution of apoptosis signal-regulating kinase 1 (ASK1)-induced apoptosis by the mitochondria-dependent caspase activation. *J. Biol. Chem.* **275**: 26576–26581.
- Holasek, S.S., Wengenack, T.M., Kandimalla, K.K., Montano, C., Gregor, D.M., Curran, G.L., and Poduslo, J.F. 2005. Activation of the stress-activated MAP kinase, p38, but not JNK in cortical motor neurons during early presymptomatic stages of amyotrophic lateral sclerosis in transgenic mice. *Brain Res.* **1045**: 185–198.
- Inoue, H., Tsukita, K., Iwasato, T., Suzuki, Y., Tomioka, M., Tateno, M., Nagao, M., Kawata, A., Saido, T.C., Miura, M., et al. 2003. The crucial role of caspase-9 in the disease progression of a transgenic ALS mouse model. *EMBO J.* **22**: 6665–6674.
- Jordan, R., Wang, L., Graczyk, T.M., Block, T.M., and Romano, P.R. 2002. Replication of a cytopathic strain of bovine viral diarrhoea virus activates PERK and induces endoplasmic reticulum stress-mediated apoptosis of MDBK cells. *J. Virol.* **76**: 9588–9599.
- Julien, J.P. and Beaulieu, J.M. 2000. Cytoskeletal abnormalities in amyotrophic lateral sclerosis: Beneficial or detrimental effects? *J. Neurol. Sci.* **180**: 7–14.
- Kikuchi, H., Almer, G., Yamashita, S., Guegan, C., Nagai, M., Xu, Z., Sosunov, A.A., McKhann, G.M.I., and Przedborski, S. 2006. Spinal cord endoplasmic reticulum stress associated with a microsomal accumulation of mutant superoxide dismutase-1 in an ALS model. *Proc. Natl. Acad. Sci.* **103**: 6025–6030.
- Kirby, J., Halligan, E., Baptista, M.J., Allen, S., Heath, P.R., Holden, H., Barber, S.C., Loynes, C.A., Wood-Allum, C.A., Lunec, J., et al. 2005. Mutant *SOD1* alters the motor neuronal transcriptome: Implications for familial ALS. *Brain* **128**: 1686–1706.
- Kopito, R.R. 1997. ER quality control: The cytoplasmic connection. *Cell* **88**: 427–430.
- Kunst, C.B., Mezey, E., Brownstein, M.J., and Patterson, D. 1997. Mutations in *SOD1* associated with amyotrophic lateral sclerosis cause novel protein interactions. *Nat. Genet.* **15**: 91–94.
- Li, M., Ona, V.O., Guegan, C., Chen, M., Jackson-Lewis, V., Andrews, L.J., Olszewski, A.J., Stieg, P.E., Lee, J.P., Przedborski, S., et al. 2000. Functional role of caspase-1 and caspase-3 in an ALS transgenic mouse model. *Science* **288**: 335–339.

- Lilley, B.N. and Ploegh, H.L. 2004. A membrane protein required for dislocation of misfolded proteins from the ER. *Nature* **429**: 834-840.
- Lilley, B.N. and Ploegh, H.L. 2005. Multiprotein complexes that link dislocation, ubiquitination, and extraction of misfolded proteins from the endoplasmic reticulum membrane. *Proc. Natl. Acad. Sci.* **102**: 14296-14301.
- Liu, J., Lillo, C., Jonsson, P.A., Vande Velde, C., Ward, C.M., Miller, T.M., Subramaniam, J.R., Rothstein, J.D., Marklund, S., Andersen, P.M., et al. 2004. Toxicity of familial ALS-linked SOD1 mutants from selective recruitment to spinal mitochondria. *Neuron* **43**: 5-17.
- Meusser, B., Hirsch, C., Jarosch, E., and Sommer, T. 2005. ERAD: The long road to destruction. *Nat. Cell Biol.* **7**: 766-772.
- Nagasawa, K., Higashi, T., Hosokawa, N., Kaufman, R.J., and Nagata, K. 2007. Simultaneous induction of the four subunits of the TRAP complex by ER stress accelerates ER degradation. *EMBO Rep.* **8**: 483-489.
- Nishitoh, H., Matsuzawa, A., Tobiume, K., Saegusa, K., Takeda, K., Inoue, K., Hori, S., Kakizuka, A., and Ichijo, H. 2002. ASK1 is essential for endoplasmic reticulum stress-induced neuronal cell death triggered by expanded polyglutamine repeats. *Genes & Dev.* **16**: 1345-1355.
- Oda, Y., Okada, T., Yoshida, H., Kaufman, R.J., Nagata, K., and Mori, K. 2006. Derlin-2 and Derlin-3 are regulated by the mammalian unfolded protein response and are required for ER-associated degradation. *J. Cell Biol.* **172**: 383-393.
- Pasinelli, P., Borchelt, D.R., Houseweart, M.K., Cleveland, D.W., and Brown Jr., R.H. 1998. Caspase-1 is activated in neural cells and tissue with amyotrophic lateral sclerosis-associated mutations in copper-zinc superoxide dismutase. *Proc. Natl. Acad. Sci.* **95**: 15763-15768.
- Pramatarova, A., Laganier, J., Roussel, J., Brisebois, K., and Rouleau, G.A. 2001. Neuron-specific expression of mutant superoxide dismutase 1 in transgenic mice does not lead to motor impairment. *J. Neurosci.* **21**: 3369-3374.
- Puttappathi, K., Wojcik, C., Rajendran, B., DeMartino, G.N., and Elliott, J.L. 2003. Aggregate formation in the spinal cord of mutant SOD1 transgenic mice is reversible and mediated by proteasomes. *J. Neurochem.* **87**: 851-860.
- Raoul, C., Estevez, A.G., Nishimune, H., Cleveland, D.W., deLapeyriere, O., Henderson, C.E., Haase, G., and Pettmann, B. 2002. Motoneuron death triggered by a specific pathway downstream of Fas: potentiation by ALS-linked SOD1 mutations. *Neuron* **35**: 1067-1083.
- Schulze, A., Standera, S., Buerger, E., Kikkert, M., van Voorden, S., Wiertz, E., Koning, F., Kloetzel, P.M., and Seeger, M. 2005. The ubiquitin-domain protein HERP forms a complex with components of the endoplasmic reticulum associated degradation pathway. *J. Mol. Biol.* **354**: 1021-1027.
- Sekine, Y., Takeda, K., and Ichijo, H. 2006. The ASK1-MAP kinase signaling in ER stress and neurodegenerative diseases. *Curr. Mol. Med.* **6**: 87-97.
- Shinder, G.A., Lacourse, M.C., Minotti, S., and Durham, H.D. 2001. Mutant Cu/Zn-superoxide dismutase proteins have altered solubility and interact with heat shock/stress proteins in models of amyotrophic lateral sclerosis. *J. Biol. Chem.* **276**: 12791-12796.
- Sifers, R.N., Brashears-Macatee, S., Kidd, V.J., Muench, H., and Woo, S.L. 1988. A frameshift mutation results in a truncated α 1-antitrypsin that is retained within the rough endoplasmic reticulum. *J. Biol. Chem.* **263**: 7330-7335.
- Suzuki, T., Park, H., and Lennarz, W.J. 2002. Cytoplasmic peptide:N-glycanase [PNGase] in eukaryotic cells: Occurrence, primary structure, and potential functions. *FASEB J.* **16**: 635-641.
- Tobisawa, S., Hozumi, Y., Arawaka, S., Koyama, S., Wada, M., Nagai, M., Aoki, M., Itoyama, Y., Goto, K., and Kato, T. 2003. Mutant SOD1 linked to familial amyotrophic lateral sclerosis, but not wild-type SOD1, induces ER stress in COS7 cells and transgenic mice. *Biochem. Biophys. Res. Commun.* **303**: 496-503.
- Tobiume, K., Matsuzawa, A., Takahashi, T., Nishitoh, H., Morita, K., Takeda, K., Minowa, O., Miyazono, K., Noda, T., and Ichijo, H. 2001. ASK1 is required for sustained activations of JNK/p38 MAP kinases and apoptosis. *EMBO Rep.* **2**: 222-228.
- Tsai, B., Ye, Y., and Rapoport, T.A. 2002. Retro-translocation of proteins from the endoplasmic reticulum into the cytosol. *Nat. Rev. Mol. Cell Biol.* **3**: 246-255.
- Urushitani, M., Kurisu, J., Tsukita, K., and Takahashi, R. 2002. Proteasomal inhibition by misfolded mutant superoxide dismutase 1 induces selective motor neuron death in familial amyotrophic lateral sclerosis. *J. Neurochem.* **83**: 1030-1042.
- Urushitani, M., Kurisu, J., Tateno, M., Hatakeyama, S., Nakayama, K., Kato, S., and Takahashi, R. 2004. CHIP promotes proteasomal degradation of familial ALS-linked mutant SOD1 by ubiquitinating Hsp/Hsc70. *J. Neurochem.* **90**: 231-244.
- Urushitani, M., Sik, A., Sakurai, T., Nukina, N., Takahashi, R., and Julien, J.P. 2006. Chromogranin-mediated secretion of mutant superoxide dismutase proteins linked to amyotrophic lateral sclerosis. *Nat. Neurosci.* **9**: 108-118.
- Veglianese, P., Lo Coco, D., Bao Cutrona, M., Magnoni, R., Pennacchini, D., Pozzi, B., Gowing, G., Julien, J.P., Tortarolo, M., and Bendotti, C. 2006. Activation of the p38MAPK cascade is associated with upregulation of TNF α receptors in the spinal motor neurons of mouse models of familial ALS. *Mol. Cell. Neurosci.* **31**: 218-231.
- Wang, J., Slunt, H., Gonzales, V., Fromholt, D., Coonfield, M., Copeland, N.G., Jenkins, N.A., and Borchelt, D.R. 2003. Copper-binding-site-null SOD1 causes ALS in transgenic mice: Aggregates of non-native SOD1 delineate a common feature. *Hum. Mol. Genet.* **12**: 2753-2764.
- Wang, J., Xu, G., Li, H., Gonzales, V., Fromholt, D., Karch, C., Copeland, N.G., Jenkins, N.A., and Borchelt, D.R. 2005. Somatodendritic accumulation of misfolded SOD1-L126Z in motor neurons mediates degeneration: α B-crystallin modulates aggregation. *Hum. Mol. Genet.* **14**: 2335-2347.
- Wengenack, T.M., Holasek, S.S., Montano, C.M., Gregor, D., Curran, G.L., and Poduslo, J.F. 2004. Activation of programmed cell death markers in ventral horn motor neurons during early presymptomatic stages of amyotrophic lateral sclerosis in a transgenic mouse model. *Brain Res.* **1027**: 73-86.
- Wong, P.C., Pardo, C.A., Borchelt, D.R., Lee, M.K., Copeland, N.G., Jenkins, N.A., Sisodia, S.S., Cleveland, D.W., and Price, D.L. 1995. An adverse property of a familial ALS-linked SOD1 mutation causes motor neuron disease characterized by vacuolar degeneration of mitochondria. *Neuron* **14**: 1105-1116.
- Yamanaka, K., Chun, S.J., Boillee, S., Fujimori-Tonou, N., Yamashita, H., Gutmann, D.H., Takahashi, R., Misawa, H., and Cleveland, D.W. 2008. Astrocytes as determinants of disease progression in inherited amyotrophic lateral sclerosis. *Nat. Neurosci.* **11**: 251-253.
- Ye, Y., Shibata, Y., Yun, C., Ron, D., and Rapoport, T.A. 2004. A membrane protein complex mediates retro-translocation from the ER lumen into the cytosol. *Nature* **429**: 841-847.

Nishitoh et al.

- Ye, Y., Shibata, Y., Kikkert, M., van Voorden, S., Wiertz, E., and Rapoport, T.A. 2005. Recruitment of the p97 ATPase and ubiquitin ligases to the site of retrotranslocation at the endoplasmic reticulum membrane. *Proc. Natl. Acad. Sci.* **102**: 14132-14138.
- Yoshihara, T., Ishigaki, S., Yamamoto, M., Liang, Y., Niwa, J., Takeuchi, H., Doyu, M., and Sobue, G. 2002. Differential expression of inflammation- and apoptosis-related genes in spinal cords of a mutant SOD1 transgenic mouse model of familial amyotrophic lateral sclerosis. *J. Neurochem.* **80**: 158-167.
- Zinszner, H., Kuroda, M., Wang, X., Batchvarova, N., Lightfoot, R.T., Remotti, H., Stevens, J.L., and Ron, D. 1998. CHOP is implicated in programmed cell death in response to impaired function of the endoplasmic reticulum. *Genes & Dev.* **12**: 982-995.

Provided for non-commercial research and education use.
Not for reproduction, distribution or commercial use.

FEBS *Letters*

The journal for rapid publication
of short reports in molecular biosciences

- ▶ RNA- and protein-folding by ribosomal proteins
- ▶ A possible prebiotic route to long polymers
- ▶ Proton channels and NADPH oxidase

Published by Elsevier on behalf of the Federation of European Biochemical Societies

Submit to: <http://www.elsevier.com/febsletters> ISSN 0014-5783
Volume 583 Number 1 5 January 2009

This article appeared in a journal published by Elsevier. The attached copy is furnished to the author for internal non-commercial research and education use, including for instruction at the authors institution and sharing with colleagues.

Other uses, including reproduction and distribution, or selling or licensing copies, or posting to personal, institutional or third party websites are prohibited.

In most cases authors are permitted to post their version of the article (e.g. in Word or Tex form) to their personal website or institutional repository. Authors requiring further information regarding Elsevier's archiving and manuscript policies are encouraged to visit:

<http://www.elsevier.com/copyright>



Silencing efficiency differs among tissues and endogenous microRNA pathway is preserved in short hairpin RNA transgenic mice

Hiroki Sasaguri^{a,c}, Tasuku Mitani^b, Masayuki Anzai^b, Takayuki Kubodera^{a,c}, Yuki Saito^a, Hiromi Yamada^a, Hidehiro Mizusawa^{a,c}, Takanori Yokota^{a,*}

^a Department of Neurology and Neurological Science, Graduate School, Tokyo Medical and Dental University, 1-5-45 Yushima, Bunkyo-ku, Tokyo 113-8519, Japan

^b Institute of Advanced Technology, Kinki University, 14-1 Minami-Akasaka, Kainan, Wakayama 642-0017, Japan

^c Twenty-First Century Center of Excellence Program on Brain Integration and Its Disorders, Tokyo Medical and Dental University, 1-5-45 Yushima, Bunkyo-ku, Tokyo 113-8519, Japan

ARTICLE INFO

Article history:

Received 28 August 2008
Revised 20 November 2008
Accepted 1 December 2008
Available online 11 December 2008

Edited by Ulrike Kutay

Keywords:

RNA interference
Short hairpin RNA
Small interfering RNA
Transgenic mice
MicroRNA
Oversaturation

ABSTRACT

In short hairpin RNA (shRNA) transgenic mice, the tissue difference in gene silencing efficiency and oversaturation of microRNA (miRNA) pathway have not been well assessed. We studied these problems in our previously-reported anti-copper/zinc superoxide dismutase (SOD1) shRNA transgenic mice. Although there was a tissue difference (liver and skeletal muscle, >95%; central nervous system and lung, ~80%), the target gene silencing was systemic and our anti-SOD1 shRNA transgenic mice recapitulated the SOD1-null mice. Neither endogenous miRNAs nor their target gene levels were altered, indicating the preservation of endogenous miRNA pathways. We think that the shRNA transgenic mice can be utilized for gene analysis.

© 2008 Federation of European Biochemical Societies. Published by Elsevier B.V. All rights reserved.

1. Introduction

RNA interference (RNAi) is evolutionally conserved sequence-specific post-transcriptional gene silencing, which is mediated by small double stranded RNA (dsRNA) [1]. The long dsRNA is cleaved by an RNase III enzyme, Dicer, in cytoplasm to generate small interfering RNA (siRNA) that is 21–23 base pair dsRNA. The target mRNA is recognized by guide (antisense) strand of the dsRNA in RNA-induced silencing complex (RISC), and is cleaved by Argonaute-2 (Ago2) protein, one of the main components of RISC [2]. This post-transcriptional gene silencing can be effectively induced by exogenously introduced siRNA or intracellularly expressed short hairpin RNA (shRNA) in mammalian cells [2,3].

The shRNA transgenic mice have been published [4–7] and expected to be an alternative method to the conventional knockout mice. For using shRNA transgenic mice as a tool for gene analysis *in vivo*, we need to know difference in silencing efficiency among tissues. Moreover, in shRNA transgenic mice, it is also important to elucidate whether microRNA (miRNA) is normally processed, because shRNA and miRNA share intracellular machineries for their maturation in mammalian cells [8–10]. We had generated anti-mouse copper/zinc superoxide dismutase (SOD1) shRNA transgenic mice, in which shRNA was ubiquitously expressed by the RNA polymerase III (Pol III) promoter [11]. Using these mice, we here evaluated the silencing efficiency in various tissues and studied endogenous miRNA pathway.

2. Materials and methods

2.1. Generation of anti-SOD1 shRNA transgenic mice

All experiments were approved by the Animal Experiment Committees of Tokyo Medical and Dental University (#0090104) and Kinki University (KAAT-19-006). We generated an anti-SOD1

Abbreviations: shRNA, short hairpin RNA; miRNA, microRNA; RNAi, RNA interference; dsRNA, double stranded RNA; RISC, RNA-induced silencing complex; Ago2, Argonaute-2; SOD1, copper/zinc superoxide dismutase; Pol III, polymerase III; ES, embryonic stem; PBS, phosphate-buffered saline; SDS, sodium dodecyl sulfate; cDNA, complementary DNA; RT-PCR, reverse transcription polymerase chain reaction; GAPDH, glyceraldehyde-3-phosphate dehydrogenase; snRNA, small nuclear RNA; AAV, adeno-associated virus

* Corresponding author. Fax: +81 3 5803 0169.

E-mail address: tak-yokota.nuro@tmd.ac.jp (T. Yokota).

shRNA expression vector and anti-SOD1 shRNA transgenic mice as reported previously [11,12]. In brief, we inserted anti-SOD1 shRNA driven by human U6 promoter into pUC19 (Takara). The shRNA expression vector was introduced into the 129/Sv embryonic stem (ES) cells (Chemicon) by electroporation. The ES cell clones in which SOD1 protein levels were effectively suppressed were introduced into C57BL/6 blastocysts (CLEA) by microinjection. We obtained F1 transgenic mice by crossing the chimeric male mice with wild-type C57BL/6 female mice.

2.2. Histological study

To analyze hepatic lipid accumulation, liver samples from 8-month-old shRNA transgenic male mice and wild-type littermates were sectioned (4 μ m) and fixed in 4% paraformaldehyde/phosphate-buffered saline (PBS) for 5 min, and then stained with filtrated Sudan III (Muto pure chemicals) at 37 °C for 30 min. Counterstaining of nuclei was performed with Mayer hematoxylin solution (Muto pure chemicals) for 3 min.

2.3. Western blot analysis

Western blot analysis was performed as reported previously [11]. Mice were killed under anesthesia with pentobarbital sodium, and perfused with cold PBS. Tissues were homogenized in the cold buffer containing 0.1% sodium dodecyl sulfate (SDS), 1% sodium deoxycholate, 1% Triton X-100, 1 mM phenylmethylsulfonyl fluoride and protease inhibitor cocktail (Sigma). Equal amounts of protein from each sample were loaded in the assays. The separated proteins were detected by specific primary antibodies; rabbit anti-SOD1 antibody (1:5000, StressGen Biotechnologies), mouse anti- β -tubulin antibody (1:1000, BD Biosciences), mouse anti-Actin antibody (1:1000, Santa Cruz Biotechnology), mouse anti-Ago2 antibody (1:500, Abcam), or rabbit anti-N-ras antibody (1:500, Santa Cruz Biotechnology).

2.4. Northern blot analysis

Northern blot analysis was performed as reported previously [11]. Ten micrograms of total RNA from each sample were loaded in the assays. The DNA probes which were used to detect RNAs were as follows; complementary DNA (cDNA) (bases 15–495) for mouse SOD1; cDNA (bases 300–614) for mouse glyceraldehyde-3-phosphate dehydrogenase (GAPDH); 5'-GGTGGAAATGAAGAAAGTAC-3' for anti-SOD1 siRNA guide strand; 5'-ACTATACAACCTAC-TACCTCA-3' for mouse let-7a; 5'-GGCATTACCGCGTGCCTTA-3' for mouse miR-124a; 5'-AAATATGGAACGCTTCACGA-3' for mouse U6 small nuclear RNA (snRNA).

2.5. Quantitative reverse transcription polymerase chain reaction (RT-PCR)

After treating with TURBO DNA-free (Ambion) to remove residual genomic DNA, 1 μ g of total RNA from each sample was reversely transcribed to cDNA using SuperScript III Reverse Transcriptase (Invitrogen). The cDNA was used for quantitative PCR with TaqMan system using the ABI Prism 7700 Sequence Detection System (Applied Biosystems) according to the manufacturer's protocol. The primers and probe used to quantify mouse SOD1 were 5'-GGTGCAGGGAACCATCCA-3' for forward primer, 5'-CCCATGCTGGCCCTTCAGT-3' for reverse primer, and 5'-AGGCA-AGCGGTGAACCACTGTGTGTTG-3' for probe. The primer and probe sets of mouse GAPDH, N-ras and N-myc were purchased from Applied Biosystems. GAPDH was used to normalize the quantitative RT-PCR values.

2.6. Laser microdissection and RNA extraction from motor neurons and non-neuronal cells

Collection of motor neurons and non-neuronal cells was performed as reported previously [13]. Spinal cords of the transgenic mice or wild-type littermates were removed and embedded in Tissue-Tek O.C.T. Compound (Sakura Finetek). Seven micrometer thick sections were mounted on a MembraneSlide (Leica) and stained with HistoGene staining solution (Arcturus). Approximate one thousand motor neurons and neighboring non-neuronal cells were dissected from the ventral horn of the lumbar spinal cord for each mouse using an AS LMD system (Leica). Total RNA was extracted using RNeasy Micro Kit (Qiagen) according to the manufacturer's protocol.

2.7. Subcellular fractionation

Subcellular fractionation was performed as described previously [14]. The cerebrum or liver was gently homogenized in cold buffer (0.22 M D-mannitol, 0.07 M sucrose, at 1 mg tissue/10 μ l buffer) with a glass-Teflon homogenizer (30 up-and-down strokes), and centrifuged at 600 \times g for 10 min. The pellets were suspended with 2.2 M sucrose and centrifuged at 40000 \times g for 1 h. The resulting pellets were used as nuclear fraction. The supernatants generated by the first centrifugation were used as cytoplasmic fraction. Total RNA was extracted using ISOGEN (Nippon Gene) for nuclear fraction and ISOGEN-LS (Nippon Gene) for cytoplasmic fraction, respectively.

2.8. Statistical analysis

Student's *t*-test was used to evaluate difference among tissues or difference between transgenic mice and wild-type littermates. Significance was set at $P < 0.05$. To compare the expression level on Western blot or Northern blot analysis, we used NIH ImageJ to quantify the band intensity.

3. Results

3.1. Anti-SOD1 shRNA transgenic mice recapitulate SOD1-null mice

As reported previously, we obtained anti-SOD1 shRNA transgenic mice (Fig. 1A) [11]. The silencing effect of the target gene was significant on both RNA and protein levels, and was stable with age and through to the F3 generation [11]. In contrast, there was no change in the expression levels of unrelated genes including GAPDH and β -actin ($P = 0.75$ and 0.27 , respectively, data not shown). The transgenic mice showed no remarkable phenotype during development. The adult mice exhibited mild fatty liver (Fig. 1B and C) and female infertility (data not shown), which were also observed in SOD1-null mice [15,16]. These findings indicate that the phenotype of the anti-SOD1 shRNA transgenic mice is similar to that of SOD1-null mice.

3.2. The siRNA-silencing efficiency differs among the tissues of the shRNA transgenic mice

We analyzed the siRNA-silencing efficiency in the various tissues of the shRNA transgenic mice. On Western blot analysis, we observed marked suppression of SOD1 protein in all the tissues examined (Fig. 2A). However, the siRNA-silencing efficiency was clearly different among the tissues; it was extremely high in the liver and skeletal muscle (>95%) and, in contrast, was relatively low in the central nervous system and lung (~80%) (Fig. 2A and B). The

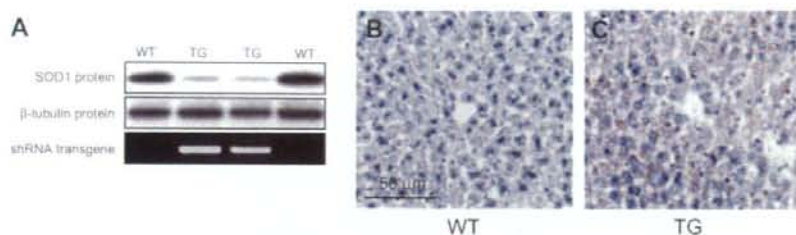


Fig. 1. Generation of anti-SOD1 shRNA transgenic mice. (A) Western blot analysis of SOD1 (upper) and β -tubulin (middle), and genomic PCR of transgene (lower) in the tails. Histological analysis in the liver of the wild-type littermates (B) and shRNA transgenic mice (C). The sections were stained with Sudan III. WT, age-matched wild-type littermates; TG, transgenic mice.

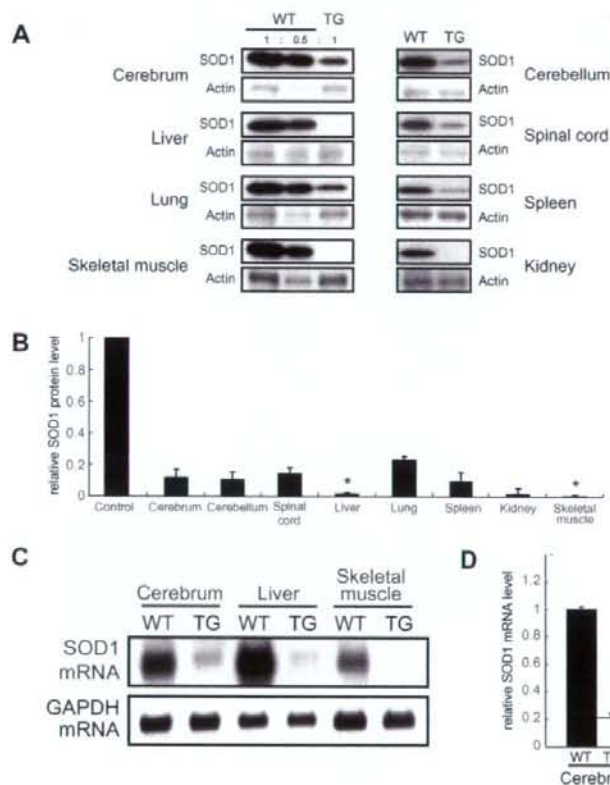


Fig. 2. Silencing efficiency in the various tissues of the shRNA transgenic mice. (A) SOD1 protein levels on Western blot analysis in the tissues of the transgenic mice. A half amount of the wild-type samples are loaded in the middle lanes of left panel to show that the signals are not saturated. (B) Quantification of their band intensities. Values are the ratio to those of age-matched wild-type littermates (mean and S.D., $n = 3$, $P < 0.05$; significance compared to cerebrum). (C) SOD1 mRNA levels on Northern blot analysis. (D) Quantitative RT-PCR of SOD1 mRNA in the cerebrum and liver. Values are the ratio to age-matched wild-type littermates (mean and S.D., $n = 3$, $P < 0.05$; significance compared to cerebrum).

difference was also confirmed on RNA level by Northern blot analysis (Fig. 2C) and quantitative RT-PCR (Fig. 2D).

3.3. The siRNA-silencing efficiency in neuronal cells is relatively lower than those in hepatocytes and muscle fibers

Because central nervous system is composed of heterogeneous cell populations, we sought to evaluate the siRNA-silencing effi-

ciency in neuronal and non-neuronal cells using laser microdissection method. The motor neurons and non-neuronal cells were isolated from the ventral horn of the lumbar spinal cords in the shRNA transgenic mice or wild-type littermates (Fig. 3A–D), and SOD1 mRNA levels were quantified by quantitative RT-PCR. The silencing efficiency in the motor neurons was approximately 80% which was similar to the non-neuronal cells (Fig. 3E) and the whole spinal cord tissue (Fig. 2B), and was less than those in the liver and

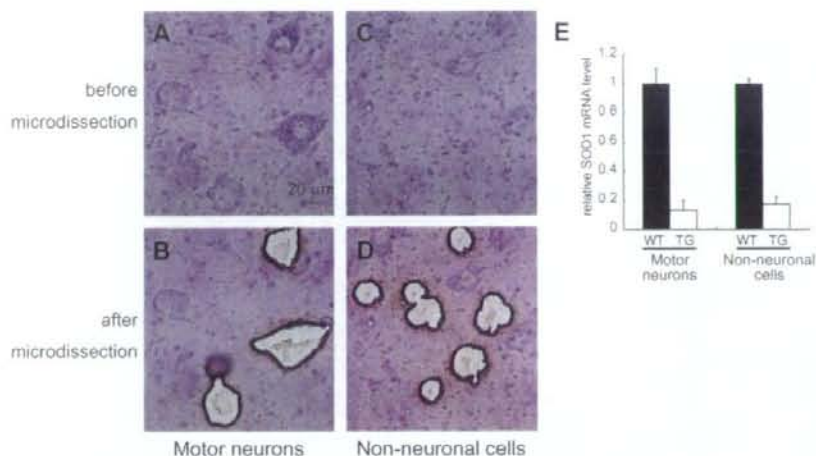


Fig. 3. Silencing efficiency in the neuronal and non-neuronal cells of the shRNA transgenic mice. (A–D) Microdissection of motor neurons and non-neuronal cells in the ventral horn of the lumbar spinal cord of the transgenic mice and age-matched wild-type littermates. Motor neurons (A and B) and non-neuronal cells (C and D) were dissected by laser microbeam. (E) Quantification of SOD1 mRNA in the motor neurons and non-neuronal cells by quantitative RT-PCR (mean and S.D., $n = 3$).

skeletal muscle (Fig. 2B). Since liver and skeletal muscle are mostly composed of hepatocytes and muscle fibers, respectively, these results indicate that the siRNA-silencing efficiency is different among cell populations in the shRNA transgenic mice.

3.4. The mechanism of tissue difference in siRNA-silencing efficiency

In order to study the mechanism of this tissue difference in siRNA-silencing efficiency, we first analyzed the expression levels of shRNA and siRNA with the probe to the guide strand of siRNA, and compared them to the expression level of the target mRNA in each tissue. The 54 mer shRNA was not detected in any tissue (data not shown), indicating that processing of shRNA by Dicer is excellent and not different among tissues. The processed guide strand of 21 mer siRNA was observed much more in the cerebrum than in the liver and skeletal muscle (Fig. 4A and B). As shown in Fig. 2C, in contrast, SOD1 mRNA level was relatively lower in the cerebrum in comparison with that in the liver. These clearly indi-

cate that relative ratio of the processed siRNA to the target mRNA in tissues does not explain the difference in siRNA-silencing efficiency.

Next, to examine whether the guide strand of siRNA properly located in the cells, we performed Northern blot analysis after subcellular fractionation of the tissue homogenates. Most of the guide strand was detected in the cytoplasmic fraction in both of the cerebrum and liver (Fig. 4C). These results show that the shRNA is similarly exported from the nucleus to the cytoplasm and that the guide strand should be similarly processed in the cytoplasm in the cerebrum and liver. These suggest that the slicer/RISC function, siRNA-cleaving ability, was lower in the cerebrum than in the liver. Therefore, we finally analyzed expression of Ago2 protein which is considered to be the slicer in mammalian cells [17]. However, the expression of Ago2 protein was not lower in the cerebrum (Fig. 4D), which was previously reported [18,19]. These findings suggest that the lower silencing efficiency in the cerebrum could not be explained by Ago2 level. The exact molecular mechanism

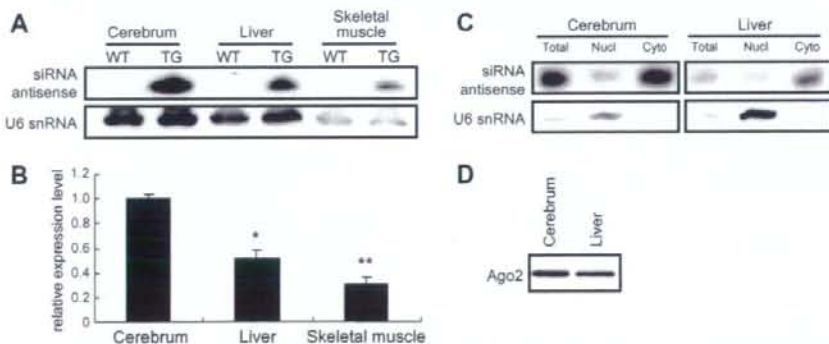


Fig. 4. The processing of shRNA/siRNA in the tissues of the transgenic mice. (A) Detection of siRNA guide strand in the cerebrum, liver and skeletal muscle on Northern blot analysis. (B) Quantification of their band intensity on Northern blot analysis. Values are the ratio to cerebrum (mean and S.D., $n = 3$, * $P < 0.05$, ** $P < 0.01$; significance compared to cerebrum). (C) Subcellular localization of the siRNA guide strand in the cerebrum and liver. U6 snRNA is used as a marker of nuclear fraction. (D) Ago2 protein in the cerebrum and liver on Western blot analysis.

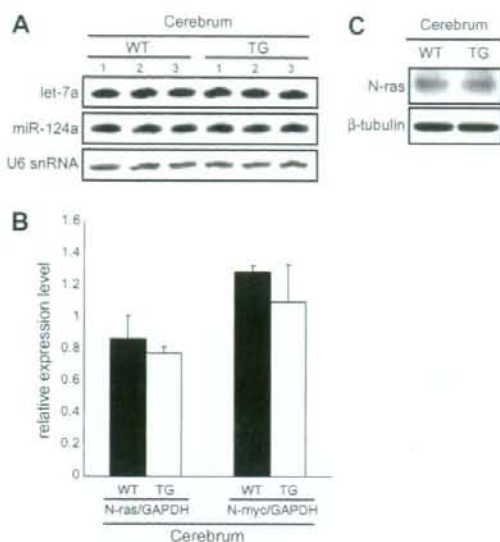


Fig. 5. Endogenous microRNA pathway in the shRNA transgenic mice. (A) Endogenous levels of miRNAs, let-7a (upper) and miR-124a (middle), in the cerebrum on Northern blot analysis. (B) Quantification of N-ras and N-myc levels, which are predicted as target genes of let-7a, in the cerebrum by quantitative RT-PCR (mean and S.D., $n = 3$). (C) N-ras protein in the cerebrum on Western blot analysis.

for the tissue difference in siRNA-silencing efficiency remains to be elucidated.

3.5. Endogenous miRNA pathway is not affected in the cerebrum of shRNA transgenic mice

To analyze whether competition between shRNA and miRNA occurred in the shRNA transgenic mice, we evaluated the expression levels of miRNAs and their target genes in the cerebrum of shRNA transgenic mice. There was no remarkable change in levels of let-7a and miR-124a on Northern blot analysis (Fig. 5A). Expression levels of N-ras and N-myc mRNAs, which were the predicted target genes of let-7a [20,21], were not altered on quantitative RT-PCR (Fig. 5B). Expression level of N-ras protein was not altered on Western blot analysis (Fig. 5C). These results clearly indicate that endogenous miRNA pathway is preserved in the shRNA transgenic mice.

The reproducibility of all results was confirmed by at least two experiments.

4. Discussion

We demonstrated the tissue difference in siRNA-silencing efficiency in the anti-SOD1 shRNA transgenic mice, but could not make clear the exact mechanism for the difference. However, the silencing effects in the tissues were generally good (>80%), and the anti-SOD1 shRNA transgenic mice could recapitulate the phenotype of fatty liver and female infertility as seen in SOD1-null mice [15,16].

Overexpression of shRNA from transgene did not induce apparent adverse effect including inhibition of endogenous miRNA pathway in our transgenic mice. It is of note that abundant shRNA/siRNA exogenously delivered by adeno-associated virus (AAV) vectors can cause drastic toxicity in the liver or brain possibly

due to oversaturation of endogenous miRNA pathway [9,22]. The absence of the toxicity in the shRNA transgenic mice is probably due to its lower expression, because such a tissue toxicity is dependent on expression level of shRNA/siRNA [9,22]. Alternatively, there might be a difference in the processing pathways between shRNA expressed from transgene and that exogenously expressed by viral vector.

In conclusion, even with tissue difference in siRNA-silencing efficiency, endogenous miRNA pathway being well preserved, the transgenic RNAi approach is considered to be a useful method for analysis of gene function in vivo.

Acknowledgements

This work was supported by Grants from the Ministry of Health Labor and Welfare, Japan (#2212065, 2212070), the 21st Century COE Program on Brain Integration and its Disorders to Tokyo Medical and Dental University.

References

- Hannon, G.J. (2002) RNA interference. *Nature* 418, 244–251.
- Dykhooorn, D.M. and Lieberman, J. (2005) The silent revolution: RNA interference as basic biology, research tool, and therapeutic. *Annu. Rev. Med.* 56, 401–423.
- Grimm, D. and Kay, M.A. (2007) Therapeutic application of RNAi: is mRNA targeting finally ready for prime time? *J. Clin. Invest.* 117, 3633–3641.
- Gao, X. and Zhang, P. (2007) Transgenic RNA interference in mice. *Physiology* 22, 161–166.
- Coumoul, X. and Deng, C.X. (2006) RNAi in mice: a promising approach to decipher gene functions in vivo. *Biochimie* 88, 637–643.
- Kunath, T., Gish, G., Lickert, H., Jones, N., Pawson, T., and Rossant, J. (2003) Transgenic RNA interference in ES cell-derived embryos recapitulates a genetic null phenotype. *Nat. Biotechnol.* 21, 559–561.
- Xia, X.G., Zhou, H., Samper, E., Melov, S. and Xu, Z. (2006) Pol II-expressed shRNA knocks down Sod2 gene expression and causes phenotypes of the gene knockout in mice. *PLoS Genet.* 2, e10.
- Rossi, J.J. (2008) Expression strategies for short hairpin RNA interference triggers. *Hum. Gene Ther.* 19, 313–317.
- Grimm, D., Streetz, K.L., Jopling, C.L., Storm, T.A., Pandey, K., Davis, C.R., Marion, P., Salazar, F. and Kay, M.A. (2006) Fatality in mice due to oversaturation of cellular microRNA/short hairpin RNA pathways. *Nature* 441, 537–541.
- Castanotto, D., Sakurai, K., Lingeman, R., Li, H., Shively, L., Aagaard, L., Soifer, H., Gagnon, A., Riggs, A. and Rossi, J.J. (2007) Combinatorial delivery of small interfering RNAs reduces RNAi efficacy by selective incorporation into RISC. *Nucleic Acids Res.* 35, 5154–5164.
- Saito, Y., Yokota, T., Mitani, T., Ito, K., Anzai, M., Miyagishi, M., Taira, K. and Mizusawa, H. (2005) Transgenic small interfering RNA halts amyotrophic lateral sclerosis in a mouse model. *J. Biol. Chem.* 280, 42826–42830.
- Yokota, T., Miyagishi, M., Hino, T., Matsumura, R., Tashiro, A., Urushitani, M., Rao, R.V., Takahashi, R., Bredesen, D.E., Taira, K. and Mizusawa, H. (2004) siRNA-based inhibition specific for mutant SOD1 with single nucleotide alternation in familial ALS, compared with ribozyme and DNA enzyme. *Biochem. Biophys. Res. Commun.* 314, 283–291.
- Ando, Y., Liang, Y., Ishigaki, S., Niwa, J., Jiang, Y., Kobayashi, Y., Yamamoto, M., Doyu, M. and Sobue, G. (2003) Caspase-1 and -3 mRNAs are differentially upregulated in motor neurons and glial cells in mutant SOD1 transgenic mouse spinal cord: a study using laser microdissection and real-time RT-PCR. *Neurochem. Res.* 28, 839–846.
- Tateno, M., Sadakata, H., Tanaka, M., Itohara, S., Shin, R.M., Miura, M., Masuda, M., Aozaki, T., Urushitani, M., Misawa, H. and Takahashi, R. (2004) Calcium-permeable AMPA receptors promote misfolding of mutant SOD1 protein and development of amyotrophic lateral sclerosis in a transgenic mouse model. *Hum. Mol. Genet.* 13, 2183–2196.
- Uchiyama, S., Shimizu, T. and Shirasawa, T. (2006) CuZn-SOD deficiency causes ApoB degradation and induces hepatic lipid accumulation by impaired lipoprotein secretion in mice. *J. Biol. Chem.* 281, 31713–31719.
- Matzuk, M.M., Dionne, L., Guo, Q., Kumar, R. and Lebovitz, R.M. (1998) Ovarian function in superoxide dismutase 1 and 2 knockout mice. *Endocrinology* 139, 4008–4011.
- Meister, G., Landthaler, M., Patkaniowska, A., Dorsett, Y., Teng, G. and Tuschli, T. (2004) Human Argonaute2 mediates RNA cleavage targeted by miRNAs and siRNAs. *Mol. Cell* 15, 185–197.
- González-González, E., López-Casas, P.P. and del Mazo, J. (2008) The expression patterns of genes involved in the RNAi pathways are tissue-dependent and differ in the germ and somatic cells of mouse testis. *Biochim. Biophys. Acta* 1779, 306–311.
- Sago, N., Omi, K., Tamura, Y., Kunugi, H., Toyooka, T., Tokunaga, K. and Hohjoh, H. (2004) RNAi induction and activation in mammalian muscle cells